

## ORIGINAL

## ARTICLE



# Serine 19 phosphorylation and 14–3–3 binding regulate phosphorylation and dephosphorylation of tyrosine hydroxylase on serine 31 and serine 40

Sadaf Ghorbani\*, Peter D. Szigetvari\* , Jan Haavik\*<sup>†</sup> and Rune Kleppe<sup>†‡</sup> 

\*Department of Biomedicine, K.G. Jebsen Centre for Research on Neuropsychiatric Disorders, University of Bergen, Bergen, Norway

<sup>†</sup>Division of Psychiatry, Haukeland University Hospital, Bergen, Norway

<sup>‡</sup>Computational Biology Unit, Department of Informatics, University of Bergen, Bergen, Norway

## Abstract

Multisite phosphorylation and structural flexibility allow for complex regulation of proteins through cellular signaling. Tyrosine hydroxylase (TH), a key enzyme of catecholamine synthesis, is regulated by multiple neuronal signaling pathways through phosphorylation at serine 19 (Ser19), serine 31 (Ser31), and serine 40 (Ser40) located in the flexible, far N-terminal region of the regulatory domain. Phosphorylated Ser19 (pSer19) provides a binding site for 14-3-3 proteins, a family of multi-target binding adaptor proteins. We hypothesized that pSer19 and 14-3-3 binding can regulate access to the Ser31 and Ser40 sites and modulate the dynamics of their phosphorylation state. To avoid complications from upstream signal interactions and have good control of TH-phosphorylation and 14-3-3 binding stoichiometry, we used purified recombinant human TH and 14-3-3 dimer types. We found that pSer19 strongly stimulated Ser31 phosphorylation (4.6-fold), but inhibited pSer31 dephosphorylation (3.4-fold).

Binding of 14-3-3 $\zeta$  counteracted the stimulatory effect of pSer19 on phosphorylation at Ser31, but amplified the effect on its dephosphorylation. In contrast, phosphorylation at Ser19 had moderate effect on pSer40 dephosphorylation, but 14-3-3 $\zeta$  binding inhibited dephosphorylation, an effect that was consistent across different homo- and heterodimeric 14-3-3s. Additional phosphorylation of Ser31 or Ser40 had little impact on the binding affinity of pSer19 TH to 14-3-3s. Mathematical modeling was performed to elucidate possible physiological implications of these observations. We propose a role of Ser19 and 14-3-3 proteins as modulators of TH phosphorylation in response to neuronal co-signaling events. These mechanisms add to our understanding of the multifaceted roles of phosphorylation and adaptor proteins in cellular signaling.

**Keywords:** 14-3-3 proteins, cross-talk, dephosphorylation, modeling, multisite phosphorylation, tyrosine hydroxylase. *J. Neurochem.* (2020) **152**, 29–47.

As a key regulatory enzyme in catecholamine biosynthesis, tyrosine hydroxylase (TH; EC 1.14.16.2; tyrosine 3-monooxygenase) (Nagatsu *et al.* 1964) is under strict control by several signaling pathways that directly target TH by Ser/Thr phosphorylation. Phosphorylation of TH can occur on several phosphorylation sites in the N-terminal regulatory domain and is mediated by a range of protein kinases. Thus, Ser19 can be phosphorylated by the Ca<sup>2+</sup>/calmodulin dependent protein kinase II (CaMKII) (Campbell *et al.* 1986), mitogen activated protein kinase activated protein kinase 2 (MAPKAP2/MK2) (Sutherland *et al.* 1993) and p38 regulated/activated protein kinase (PRAK/MK5) (Toska

Received June 28, 2019; revised manuscript received August 27, 2019; accepted August 29, 2019.

Address correspondence and reprint requests to Rune Kleppe, Computational Biology Unit, Department of Informatics, Thormøhlens gate 55, 5020 Bergen, Norway. E-mail: rune.kleppe@uib.no

**Abbreviations used:** aa, amino acid; CDK5, cyclin-dependent kinase 5; cPP, cellular protein phosphatases; PKA, cAMP dependent protein kinase; pNP, pure non-specific phosphatase; PRAK, p38-regulated/activated protein kinase; SPR, surface plasmon resonance; TH, tyrosine hydroxylase; TH-pS19, TH phosphorylated on Ser19; TH-pS19pSer31, TH phosphorylated on both Ser19 and Ser31; TH-pS19pSer40, TH phosphorylated on both Ser19 and Ser40; TH-pS31, TH phosphorylated on Ser31; TH-pS40, TH phosphorylated at Ser40.

*et al.* 2002); TH Ser31 (amino acid (aa) sequence of hTH1) phosphorylation is mediated by MAPK1/2 (ERK1/2) (Haycock *et al.* 1992) and the cyclin-dependent protein kinase 5 (CDK5) (Moy and Tsai 2004; Kansy *et al.* 2004); TH Ser40 (aa sequence of hTH1) phosphorylation is reported for cAMP- and cGMP-dependent protein kinases (PKA and PKG, respectively) (Campbell *et al.* 1986; Roskoski *et al.* 1987; Rodríguez-Pascual *et al.* 1999), Protein Kinase C (Albert *et al.* 1984; Funakoshi *et al.* 1991), CaMKII, MAPKAPK (1 and 2) (Sutherland *et al.* 1993), and Mitogen and stress-activated protein kinase 1 (Toska *et al.* 2002; Dunkley *et al.* 2004). Phosphorylated TH at Ser/Thr 8 was also reported by MAPK1/2 (Haycock 1990) although other kinases may target this site as well.

Phosphorylation of TH is known to alter its enzyme kinetic properties. Thus, phosphorylation of Ser40 is the most potent for activation of TH in the presence of catecholamines (Almas *et al.* 1992; Daubner *et al.* 2011), whereas phosphorylation at Ser31 has more moderate effects on TH activity and Ser/Thr8 has no reported effect (Sutherland *et al.* 1993; Lindgren *et al.* 2002). It is recently reported that Ser31 phosphorylation is involved in the localization of TH with Golgi and synaptic like vesicles, probably through the interaction with vesicular monoamine transporter and  $\alpha$ -synuclein (Jorge-Finnigan *et al.* 2017). The Ser31 site may therefore be involved in compartmentalization and trafficking of TH.

The activation of TH by Ser19 phosphorylation is reported to depend on 14-3-3 binding, whereas Ser19 phosphorylation alone has little effect on the activity of TH *in vitro* (Itagaki *et al.* 1999; Toska *et al.* 2002). Phosphorylation-dependent interaction with 14-3-3 proteins has also been implicated in the control of TH stability and interaction with membranes (Yamauchi *et al.* 1981; Itagaki *et al.* 1999; Obsilova *et al.* 2008; Halskau *et al.* 2009). The 14-3-3 proteins are a highly conserved family of regulatory proteins that mainly exist as homo- or heterodimers and are highly abundant in the brain (Fu *et al.* 2000).

The phospho-state of TH is determined by the competing rates of phosphorylation and dephosphorylation. The dephosphorylation of phospho-Ser40 (pSer40) is quite well studied (Leal *et al.* 2002; Bevilaqua *et al.* 2003) (Fig. 1). The protein phosphatase 2A (PP2A) complex is a potent phosphatase for pSer40, whereas protein phosphatase 1 or the calcium regulated protein phosphatase 2B show little efficacy toward this site (Bevilaqua *et al.* 2003). However, in chromaffin cells the protein phosphatase 2C complex was also found to be an efficient TH pSer40 phosphatase, especially at higher TH levels (Bevilaqua *et al.* 2003; Bevilaqua *et al.* 2003). PP2A-type (okadaic acid sensitive) phosphatase activity toward TH phospho-Ser19 (pSer19) or phospho-Ser31 (pSer31) has been reported (Leal *et al.* 2002), however, its relative efficacy toward the dephosphorylation rate at different sites is not well understood.

As TH is a homo-tetramer, the number of possible different phospho-states is quite substantial. However, it is still unclear if any particular multisite phospho-states of TH have a special physiological role beyond that found for the sites separately. The closely spaced phosphorylation sites within the N-terminal regulatory domain have been shown to affect each other through hierarchical phosphorylation, in what is believed to be caused by intra-subunit conformational changes (Bevilaqua *et al.* 2001). Thus, phosphorylation of Ser19 or Ser31 increases the rate of Ser40 phosphorylation by PKA about two- and ninefold, respectively (Bevilaqua *et al.* 2001; Lehmann *et al.* 2006). Cellular studies support the relevance of these effects during signal-mediated phosphorylation of TH (Bobrovskaya *et al.* 2004; Lehmann *et al.* 2006). It is however unclear if the observed increase in Ser40 phosphorylated TH (TH-pS40) by pSer19 stimulation in cells is caused only by the hierarchical effect on phosphorylation or if additional effects are present, such as decreased dephosphorylation rate or protein localization and interaction. Binding of 14-3-3 proteins to pSer19 may influence the TH phosphorylation and dephosphorylation of other sites (Kleppe *et al.* 2014b). While the effect of Ser19 on Ser40 is recognized, the influence of Ser19 phosphorylation on Ser31 remains unknown.

We provide here a more detailed investigation about how Ser19 phosphorylation modulates the phospho-state of Ser31 and Ser40, also how 14-3-3 proteins assist in regulation of both Ser31 and Ser40 phosphorylation and dephosphorylation. We found that both phosphorylated Ser19 itself and binding of 14-3-3 proteins altered the kinetics of phosphorylation and dephosphorylation of Ser31 in particular, but also for Ser40. We did not find any effect of Ser31 or Ser40 phosphorylation on the binding affinity of different 14-3-3 dimers to TH-pSer19, suggesting that these sites are not contributing much to the binding. Partial accessibility of Ser19 was found in the 14-3-3:TH complex, suggesting the occurrence multiple conformational states of the complex. Using modeling we elucidate the possibility of 14-3-3 mediated multisite cross-talk in the case of 14-3-3 complexes with partial accessibility for kinase and phosphatases. Our results suggest that Ser19 phosphorylation and 14-3-3 binding act to modulate the phosphorylation dynamics of Ser31 and Ser40 sites.

## Materials and methods

### Materials

[<sup>32</sup>P- $\gamma$ ] ATP was from PerkinElmer (Georgia, USA). pGEX-2T plasmids for expression of 14-3-3 $\gamma$ ,  $\eta$ , and  $\zeta$  were gifts from Prof. Alastair Aitken (Edinburgh, UK), for 14-3-3 $\beta$  from Dr C. James Hastie [MRC, Division of Signal Transduction Therapy, University of Dundee (Scotland)] and pET11 for expression of his-tagged 14-3-3 $\epsilon$  was from Prof. S.O. Døskeland (Department of Biomedicine, University of Bergen). Active p38-regulated/activated protein kinase (PRAK) was from University of Dundee, MRC PPU Reagents and

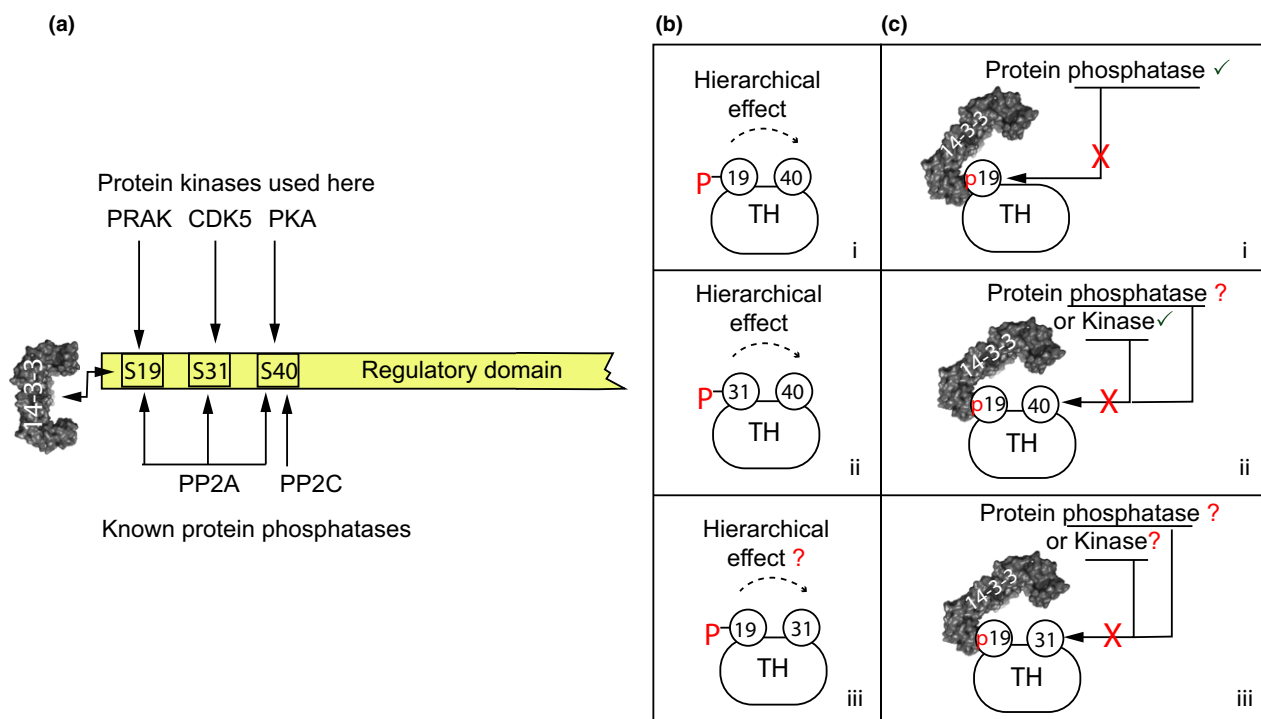


**Fig. 1** Illustration of TH phosphorylation and site cross-talk. (a) Illustration of kinases used and phosphatases that target Ser19, Ser31, and Ser40 of TH. (b) Panels i) and ii) illustrate the cross-talk between pSer19 and Ser40 as well as pSer31 and Ser40 that leads to an increase in Ser40 phosphorylation. Panel iii) illustrates the unknown

cross-talk between pSer19 and Ser31. (c) Possible scenarios of how binding of 14-3-3 proteins (grey) can influence TH phosphorylation-state at Ser19, Ser31, and Ser40 by affecting the accessibility of these sites for the protein kinases and phosphatases.

Services. Cyclin-dependent protein kinase 5 (Cdk5/p35 Protein) was from Merck Millipore (Darmstadt, Germany). Protease inhibitor tablets (complete) were from Roche Molecular Biochemicals (Indianapolis, IN, USA). Unless otherwise stated, reagents were from Sigma-Aldrich (St. Louis, MO, USA). Shrimp alkaline phosphatase was from New England Biolabs. GST capture kit and CM5 chips were from GE Healthcare Life Science. The custom-made materials will be shared upon reasonable request.

#### Expression and purification of proteins

Human TH1 was expressed as a (His)<sub>6</sub>-ZZ-hTH1 fusion protein in *E. coli* (BL21 Codon Plus (DE3), Stratagene, CA, US) using the pET-ZZ-1a vector (Bezem *et al.* 2016) and purified using Ni-NTA metal affinity resin (Clontech, CA, US) before the affinity tag was removed by TEV protease cleavage. The preparation was checked by SDS-PAGE for homogeneity and complete removal of His-tag and the tetrameric hTH1 was isolated using size exclusion chromatography (Superdex 200 10/300 GL) (Fig. S1). The purified proteins were tested for presence of LPS using a chromogenic endotoxin quantification kit (A39552S, Pierce, Thermo Fisher Scientific, Waltham, MA, USA), and up to 5 pg LPS/μg TH protein was found. His-tagged 14-3-3ε was expressed in *E. coli* using the pET11 expression vector and purification using Ni-NTA according to manufacturer's protocols. GST-fused 14-3-3 isoforms (β, γ, η, ζ) were expressed in *E. coli* (BL21-CodonPlusDE3) and purified as described (Kleppe *et al.* 2014b; Ghorbani *et al.* 2016). For

production of homodimeric 14-3-3β/γ/η/ζ the GST-fusion protein was cleaved on the glutathione sepharose column and the 14-3-3 dimers were eluted and further purified on gel filtration (Superdex 200 10/300 GL). Heterodimeric forms of 14-3-3ε were isolated using a combination of GST- and His-tag affinity purification as described (Ghorbani *et al.* 2016). SDS PAGE and gel filtration profiles showing the purity and different steps of the isolation procedure can be found in the supplementary (Fig. S2). The uncleaved GST-14-3-3s were used for Surface plasmon resonance measurements. We have previously found only minor differences in the kinetic values between GST-14-3-3 or immobilized 14-3-3 in their binding to phosphorylated TH (Kleppe *et al.*, 2014b). We have earlier performed native MS measurements of our purified 14-3-3 preparations, confirming exactly the expected mass of the dimers (Kleppe *et al.* 2014b). These experiments verified the absence of co-purified contaminants despite the sticky-ness of these proteins. The catalytic subunit of PKA was purified from bovine heart as described previously (Kopperud *et al.* 2002) and was kindly provided by Prof. S.O. Døskeland (Department of Biomedicine, University of Bergen).

#### TH phosphorylation assays

For affinity and dephosphorylation studies phosphorylation of Ser19 and 40 were performed as described previously (Kleppe *et al.* 2014b; Ghorbani *et al.* 2016). For affinity studies TH (2 mg/mL) in HEPES buffer (25 mM Hepes, pH 7.2, 130 mM KCl, 0.1 mM

EGTA, 10 % glycerol, 1 mM DTT) was incubated at 25°C in presence of active PRAK (7.5 U/mL) or the catalytic subunit of PKA (100 nM), to prepare TH phosphorylated at Ser19 or Ser40, respectively. The phosphorylation reaction was started by addition of ATP (0.5 mM) and MgCl<sub>2</sub> (5 mM). Ser31 was phosphorylated using CDK5 (25 U/μL) at 25°C in MOPS (8 mM) buffer pH 7.0 containing EDTA (0.2 mM), ATP (0.5 mM), MgCl<sub>2</sub> (5 mM). Double phosphorylated samples were prepared by sequential phosphorylation of TH by PRAK and PKA or CDK5. The assay duration was set to gain full stoichiometry. To measure the stoichiometry of phosphorylation a parallel sample was mixed with radiolabeled phosphate (0.01 mCi [<sup>32</sup>P]-γ-ATP) 4 μL aliquots were taken at different time points, spotted on phospho-cellulose paper and rinsed in orthophosphoric acid before measuring labeled protein by scintillation counting. Samples for dephosphorylation assays were prepared the same as mentioned above except that the ATP mix contained [<sup>32</sup>P]-γ-ATP to radiolabel phosphorylated TH. For phosphorylation rate studies, Ser40 and Ser31 were phosphorylated using 2 nM PKA and 3 or 15 U/μL CDK5.

#### PC12 cell lysate preparation

The cell line was purchased from ATCC® (PC-12-1721™; RRID: CVCL\_0481A). To the best of our knowledge, this cell line is not listed as a commonly misidentified cell line by the International Cell Line Authentication Committee. The maximum number of passages for cell line was five passages from a purchased vial of cells. The cells were not authenticated as the passage number was low and the cells were purchased from the company directly. To prepare PC12 cell lysate, a cell pellet containing about  $7 \times 10^6$  cells were dissolved in 200 μL lysis buffer [50 mM HEPES pH 7.4, 1 mM EDTA, 1 mM DTT, 1 mM EGTA, 0.1 % Triton, 2x protease inhibitor cocktail (Complete EDTA-free, Roche)] and incubated on ice for 15 min then centrifuged at 18 000 g for 10 min to remove cell debris. To remove small metabolites, the supernatant was washed two times with lysis buffer (without triton) in 500 μL spin-filter tubes (Amicon Ultra-0.5, 30 000 MWCO). The final wash was with 25 mM K-HEPES pH 7.0, 1 mM DTT and 1x protease inhibitor. The lysate was concentrated to about 100 μL, aliquoted and stored at -80°C. The protein concentration of the lysate was measured by Direct detect (Merck Millipore).

#### TH dephosphorylation

We measured dephosphorylation rates of Ser40, Ser19, and Ser31, labeled by radioactive phosphate, using either recombinant purified and non-specific phosphatase (pNP, Shrimp alkaline phosphatase) or intact, endogenous cellular protein phosphatases (cPP) present in lysates from PC-12 cells as previously described (Kleppe *et al.* 2014b; Ghorbani *et al.* 2016).

#### Enzymatic activity assays of phospho-variants

Purified batches of phosphorylated human TH1 were first subjected to a controlled dephosphorylation experiment. There, two aliquots of each phospho-variant were mixed 1 : 1 with buffer containing 25 mM Na-HEPES (pH 7.4), 130 mM KCl, 1 mM EDTA, 1 mM EGTA, 1 mM DTT and either 1 U shrimp alkaline phosphatase or the storage buffer without the enzyme (25 mM TRIS-HCl (pH 7.5), 1 mM MgCl<sub>2</sub>, 50 % glycerol). The dephosphorylation reaction was completed after 10 min at 25°C. TH concentration within the

aliquots was monitored using NanoDrop 2000 (Thermo Fisher Scientific, Waltham, MA, USA) before and after the reaction and the data was later normalized for minor differences between the phosphorylated and dephosphorylated samples. The addition of phosphatase did not affect overall protein concentrations.

All phospho-variants were injected into identical reaction mixtures that comprised of 100 mM Na-HEPES (pH 7.0), 100 μM (NH<sub>4</sub>)<sub>2</sub>Fe(SO<sub>4</sub>)<sub>2</sub>, 50 μg/mL catalase, 500 μg/mL BSA, and 25 μM L-tyrosine. 14-3-3γ was present in selected assays in a ~4 : 1 ratio with TH (60 μg/mL). The reactions were initiated at 37°C with the addition of 20 μM BH4, 2 mM DTT and stopped with 1 : 1 v/v chilled EtOH-HAc (pH 4.0). L-DOPA formation was detected using fluorometric detection techniques (Fossbakk *et al.* 2014). The significances of differences were evaluated by two-tailed Welch's *t*-tests within the Prism 7.0 software environment (GraphPad Software Inc., San Diego, CA, USA).

#### Surface plasmon resonance measurements

The interaction between phosphorylated TH and 14-3-3 proteins was measured using a Biacore 3000 (Uppsala, Sweden) instrument as described previously (Kleppe *et al.* 2014b; Ghorbani *et al.* 2016). In brief, the GST-14-3-3 proteins were immobilized on a CM5 chip using a GST capture kit according to manufacturer's instructions. We have previously shown that there are only minor differences in the binding kinetics of TH to immobilized GST-14-3-3 proteins compared to the immobilized non-fusion 14-3-3 proteins (Kleppe *et al.* 2014b). 14-3-3ε:ε was immobilized using direct amine coupling (10 mM Na-acetate, pH 5.4). All binding studies were performed using standard HBS-P buffer at flow of 30 μL/min, at 25°C. Sensograms were analyzed using the BIAevaluation v2.2 program by non-linear curve fitting as described (Kleppe *et al.* 2014b).

#### Mathematical modeling

We performed simple mathematical modeling to investigate if the reported *in vitro* hierarchical phosphorylation of TH between Ser19 and Ser40 could explain cellular observations of TH phosphorylation stoichiometry for Ser40 in the presence or absence of Ser19 stimulation. Both linear kinetics and non-linear Michaelis–Menten kinetics were investigated for kinase and phosphatase. At steady state the rate ratios of kinase over phosphatase can be estimated for Ser40 based on the observed stoichiometry at basal and PKA-stimulated conditions, in absence of Ser19 stimulation and used to calculate the expected increase at conditions of stimulated Ser19 phosphorylation. The modeled effect of Ser19 stimulated phosphorylation was based on the inter-subunit mechanism reported, with a threefold increased rate of PKA mediated of Ser40 phosphorylation for subunits of TH where Ser19 was also phosphorylated (see supplemental text for details).

Modeling was also used to investigate conditions where 14-3-3 proteins could modulate the phosphorylation state of a (functional) site distant from the phospho-recognition site (gate-keeper site) of 14-3-3, but that becomes partially covered by 14-3-3 binding. The approach was the same as used previously for modeling 14-3-3 phospho-modulation of target proteins (Kleppe *et al.* 2014a), using ordinary differential equations and numerical integration in Copasi (4.19) (Hoops *et al.* 2006). It assumes that most cellular 14-3-3 is associated with high and low affinity binding proteins that will have

a buffering effect on the 14-3-3 availability. We here specifically modeled the effect of partial access to the functional site for kinase and phosphatase (see supplemental text for details).

### Statistical analysis and study design

The two-tailed Student's *t*-test and Welch's two-tailed *t*-test were used to evaluate significant differences between the samples. Each value is given as mean  $\pm$  SD or SEM from three different *in vitro* assays, with statistical significance stated in figure legends. Holm-Bonferroni correction was used when multiple testing was performed. For analysis of association and dissociation kinetics single factor ANOVA test was used and the  $\chi^2$  values for the fits are given. Researchers were not blinded to the experimental conditions and the experimental data were not randomized. Sample sizes were not statistically pre-determined and there was no outlier removal. We did not perform sample calculation or test for normality.

### Ethical approval

No institutional or ethical approval was needed for this study.

## Results

### Phosphorylation of Ser19 site stimulates phosphorylation of Ser31 only in absence of 14-3-3 proteins

As pSer19 has previously been shown to stimulate Ser40 phosphorylation we tested first if 14-3-3 $\zeta$  influenced PKA mediated phosphorylation of this site. Pre-incubation of TH-pS19 in the presence of 14-3-3 $\zeta$  gave a twofold lower rate of PKA phosphorylation compared to TH-pS19 pre-incubated in the absence of 14-3-3 (Fig. 2a). As Ser31 is located in even closer vicinity to Ser19 than Ser40 in the primary structure, we tested if there was a similar stimulatory effect of pSer19 on the rate of Ser31 phosphorylation. Using CDK5 as a kinase, we found a 4.6-fold increase in the rate of Ser31 phosphorylation when Ser19 was previously phosphorylated with PRAK, compared to a control TH that was treated the same, but without PRAK phosphorylation (Fig. 2b). We further tested if 14-3-3 $\zeta$  binding influenced the pSer19 crosstalk to Ser31, as was found for Ser40. TH pre-phosphorylated with PRAK to yield TH-pS19, was subsequently phosphorylated on Ser31 using CDK5 in presence or absence of a pre-incubation with 14-3-3 $\zeta$  (Fig. 2c). The results showed that the initial rate of Ser31 phosphorylation was significantly decreased upon 14-3-3 $\zeta$  binding to TH-pS19 (4.7-fold), eliminating the stimulatory effect of pSer19 on Ser31.

### The presence of phosphorylated Ser19 slows down dephosphorylation of Ser31

Major TH Ser/Thr phosphatases for the Ser40 site are protein phosphatase 2A (PP2A) and 2C (PP2C) (Haavik *et al.* 1989; Leal *et al.* 2002; Bevilaqua *et al.* 2003), but less is known about the key phosphatases for the other sites and for multi-phosphorylated TH. To mimic the dephosphorylation of TH in cells, we used cell lysate (centrifuged (18 000 g) and

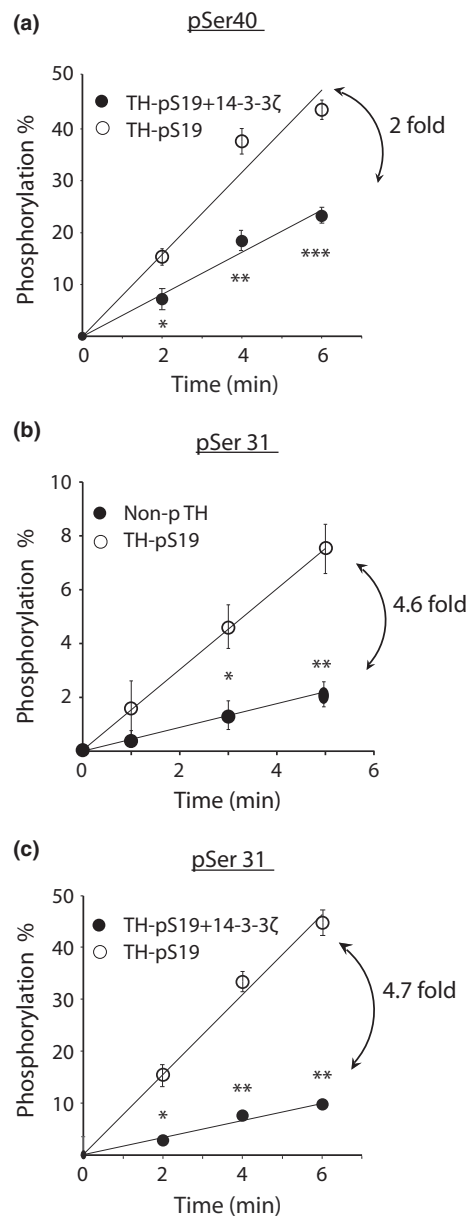


**Fig. 2** The hierarchical effect of Ser19 on Ser31 and Ser40 phosphorylation is abolished by 14-3-3 $\zeta$ . Phosphorylation of the Ser40 or Ser31 sites was measured. In (a) PKA (2 nM) mediated Ser40 phosphorylation was measured for TH-pS19 (2  $\mu$ M, phosphorylation stoichiometry  $1.0 \pm 0.01$ ) in the absence (○) or presence (●) of 14-3-3 $\zeta$  (10  $\mu$ M). In (b) the hierarchical effect from pSer19 was tested on Ser31 phosphorylation using CDK5 (3 U/ $\mu$ L) for phosphorylation of TH (2  $\mu$ M) in absence (●) or presence (○) of Ser19 pre-phosphorylation (stoichiometry  $1.0 \pm 0.01$ ). In (c) CDK5 (15 U/ $\mu$ L) mediated Ser31 phosphorylation of TH-pS19 (2  $\mu$ M, phosphorylation stoichiometry  $1.0 \pm 0.01$ ) was measured in the absence (○) or presence (●) of 14-3-3 $\zeta$  (10  $\mu$ M). Statistical significance was determined by two-tailed *t*-test ( $n = 3$  (three different *in vitro* assay experiments), average  $\pm$  SD); \* $0.002 < p < 0.008$ ; \*\* $0.0001 < p < 0.0006$ ; \*\*\* $p < 5 \times 10^{-5}$

metabolite-free) from PC-12 cells that should contain intact, relevant, protein complexes of these protein phosphatases (cPP) (Bevilaqua *et al.* 2003; Ghorbani *et al.* 2016). This lysate contained rat TH at a total concentration of about  $0.11 \pm 0.02$  ng/ $\mu$ L (Fig. S3). The ratio of rat TH (0.33 ng) to recombinant human TH (3.4  $\mu$ g) in our assays was therefore about 1 to 10 000, and any possible influence from rat TH could be ignored. Using cPP, we compared the dephosphorylation of TH labeled on different sites. We also investigated the possible impact of pSer19 on the dephosphorylation of Ser31 and Ser40. The different sites were labeled to stoichiometries of  $1.0 \pm 0.01$ ,  $1.0 \pm 0.04$ , and  $0.7 \pm 0.02$  for Ser19, Ser31, and Ser40, respectively, and their remaining phosphorylation was measured at different time points after adding the lysate (Fig. 3). At the same TH (2  $\mu$ M) and lysate concentration, the three sites were

dephosphorylated at different rates by okadaic acid-sensitive phosphatases. For Ser19 there was 13.5 % remaining phosphatase activity after treatment with high dose okadaic acid (2  $\mu$ M) and there was only very moderate effect from pre-treatment with the 14-3-3 inhibitor R18 (25  $\mu$ M), suggesting that possible 14-3-3 proteins in the lysate do not influence the measurements (Fig. 3a,e).

The Ser31 site was dephosphorylated more rapidly than Ser19 (2.8-fold), in all likelihood by PP2A type activity as dephosphorylation was very efficiently inhibited by okadaic acid, with only 2.5 % remaining activity (Fig. 3b,e). Interestingly, when Ser19 was also phosphorylated, the dephosphorylation rate of Ser31 was decreased by 70 %. Addition of equal amounts of Ser19 phosphorylated TH to single Ser31 phosphorylated TH only partially inhibited Ser31 dephosphorylation (Fig. 3c). Also, addition of R18 to

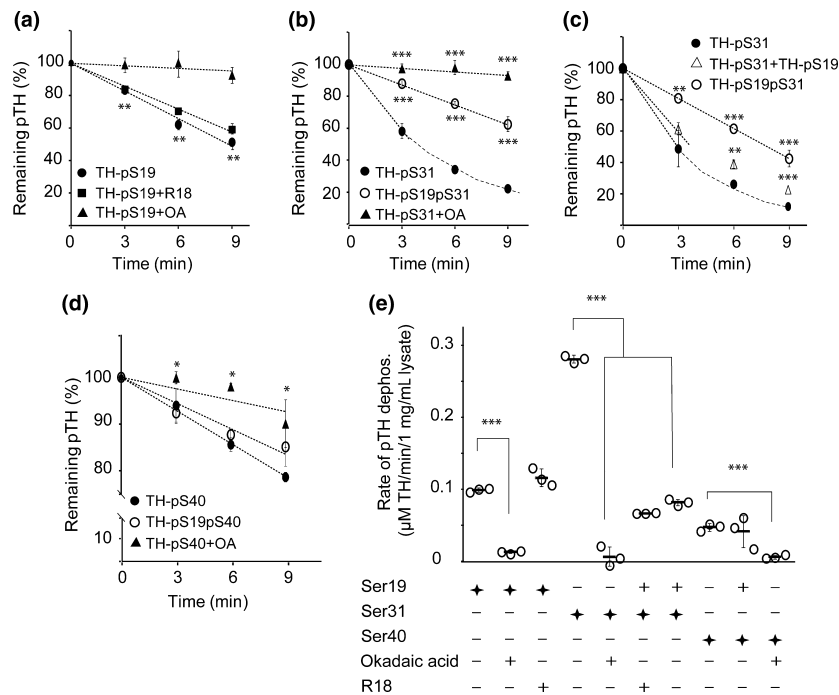


**Fig. 3** Dephosphorylation of TH at different sites by PC-12 protein phosphatases. Dephosphorylation of single- or double-phosphorylated TH (2  $\mu$ M) was measured in presence or absence of either R18 (25  $\mu$ M) or okadaic acid (OA, 2  $\mu$ M). TH was incubated with 1 mg/mL PC-12 cell lysate as described in Methods. (a) phospho-Ser19 dephosphorylated in TH-pS19 (stoichiometry:  $1.0 \pm 0.01$ ) (●) alone, in presence of R18 (■) and okadaic acid (▲) (*p*-values evaluated for TH-pS19 vs TH-pS19 + OA). (b) shows the dephosphorylation of phospho-Ser31 for TH-pS31 (stoichiometry:  $1.0 \pm 0.01$ ) alone (●), in presence of okadaic acid (▲) and for TH pre-phosphorylated on Ser19 and Ser31 (TH-pS19pS31, stoichiometry for Ser19 and Ser31 was  $1.0 \pm 0.01$  and  $1.0 \pm 0.04$ , respectively) (○) (*p*-values evaluated for TH-pS31 vs TH-pS31 + OA and TH-pS31 vs. TH-pS19pS31). (c) shows pSer31 dephosphorylation in TH-pS31 (1  $\mu$ M, ●), TH-

pS19pS31 (1  $\mu$ M, ○) and a mixture of TH-pS31 and TH-pS19 (1  $\mu$ M, △) (*p*-values evaluated for TH-pS31 vs TH-pS31 + TH-pS19 and for TH-pS31 vs TH-pS19pS31). (d) shows phospho-Ser40 dephosphorylation of TH-pS40 (stoichiometry:  $1.0 \pm 0.01$ ) (●), of TH-pS40 in the presence of okadaic acid (▲) and of double phosphorylated TH (TH-pS19pS40, stoichiometry for Ser19 and Ser40 was  $1.0 \pm 0.01$  and  $0.7 \pm 0.02$ , respectively) (○) (*p*-values evaluated for TH-pS40 vs. TH-pS19pS40). (e) shows a comparison of dephosphorylation rates of TH at different sites for single- and Ser19-double-phosphorylated states. (→) shows the sites that were labeled radioactively. The individual data points are shown, as well as average  $\pm$  SD. Statistical significance was determined by two-tailed *t*-test ( $n = 3$  (three different *in vitro* assay experiments), average  $\pm$  SD). \**p* = 0.01; \*\* $0.001 < p < 0.009$ ; \*\*\**p* < 0.0006.

the lysate prior to dephosphorylation had no effect (Fig. 3e). Using a purified non-specific phosphatase (pNP), the rate of pSer31 dephosphorylation was the same whether Ser19 was phosphorylated or not (data not shown).

The dephosphorylation rate of Ser40 was the slowest of all sites, 50 % and 17 % that of Ser19 and Ser31, respectively (Fig. 3d,e). As expected, the majority of the phosphatase activity towards TH-pS40 was inhibited by okadaic acid, with about 14 % residual activity remaining. Dephosphorylation of Ser40 was also slightly inhibited (13 %) by the combined Ser19 phosphorylation.

### 14-3-3 proteins inhibit the dephosphorylation of the Ser31 and Ser40 sites

As binding of 14-3-3 proteins to TH-pS19 was found to inhibit phosphorylation, we tested the effect of 14-3-3 binding on pSer31 and pSer40 dephosphorylation. We first investigated the effect on double-phosphorylated TH (TH-pS19pS40), where only Ser40 was labeled radioactively. Using pNP for dephosphorylation, we found linear kinetics and a substantial inhibitory effect of 14-3-3 $\zeta$  on the rate of pSer40 dephosphorylation (4.4-fold slower) (Fig. 4a). Testing many different 14-3-3 dimer types, homo- and heterodimers of 14-3-3 $\epsilon$ , we found that all 14-3-3s had an inhibitory effect on the rate of pNP-mediated pSer40 dephosphorylation of TH-pS19pS40 (Fig. 4b). A decline in rate between 52 and 72 % was found, where 14-3-3 $\zeta$  and 14-3-3 $\eta$  homodimers seemed to have the weakest and the strongest effect, respectively. When using PC-12 lysate as the source of native phosphatase (Fig. 4c,d), we observed linear kinetics and 14-3-3 $\zeta$  inhibited the pSer40 dephosphorylation of TH-pS19pS40, although less prominently (2.8-fold) than what was observed for the pNP phosphatase (Fig. 4c). We also found the inhibition of pSer40 dephosphorylation by other 14-3-3 dimer types, ranging between 31 and 63 % (Fig. 4d). Heterodimers of 14-3-3 $\epsilon$  and homodimeric 14-3-3 $\gamma$  had the largest effect, and homo-dimeric 14-3-3 $\zeta$  and  $\eta$  had the lowest (Fig. 4d). We found no significant effect of 14-3-3 proteins on dephosphorylation of TH-pS40 by the cPP (Fig. S4), which fits with the lack of substantial binding of these 14-3-3 dimers to TH-pS40 (Kleppe *et al.* 2014b) and suggesting that 14-3-3 did not directly affect the activity of the phosphatases in the lysate.

We next investigated the impact of 14-3-3 $\zeta$  on the dephosphorylation of pSer31 in TH-pS19pS31, using pNP (Fig. 5a) or cPP (Fig. 5b) as phosphatase. The effect of 14-3-3 $\zeta$  was more pronounced for pSer31 than what we observed for pSer40, showing a 6.9- and 3.7-fold lower rate of pSer31 dephosphorylation using pNP or cPP, respectively.

### Multisite phosphorylation has only moderate effects on 14-3-3 binding to TH

Phosphorylation of TH at Ser19 has been shown to be crucial for its binding to mammalian 14-3-3 proteins (Itagaki *et al.*

1999; Kleppe *et al.* 2001; Halskau *et al.* 2009) and we have recently reported similar binding affinity of different 14-3-3 dimer types for TH-pS19 (Ghorbani *et al.* 2016). We wanted to test if increased binding or different binding modes of 14-3-3 proteins were involved in the observed inhibition of TH Ser31 and Ser40 dephosphorylation and phosphorylation by 14-3-3 proteins. We first measured if Ser40 phosphorylation affected the binding kinetics of TH to any of the 14-3-3 dimer types. TH was phosphorylated on Ser19 (PRAK) or Ser40 (PKA) and the association and dissociation kinetics were measured for different 14-3-3 isoform homodimers and their heterodimers with 14-3-3 $\epsilon$  (Fig. 6a, Table 1). We found no binding of TH-pS40 to any of the 14-3-3 dimers at TH concentrations < 1  $\mu$ M. Compared to recently published results on binding of 14-3-3s to TH-pS19 (Ghorbani *et al.* 2016), the largest difference was observed for binding of the 14-3-3 $\epsilon$ : $\zeta$  heterodimer, where a 3-fold affinity difference was estimated (Table 1). The 14-3-3 $\epsilon$ : $\zeta$  heterodimer showed the highest binding affinity for TH-pS19pS40 ( $K_d \sim 1.2$  nM). The rate constants of the 14-3-3:TH complex showed more variation among 14-3-3 dimers than the computed equilibrium dissociation constant ( $K_d = k_d/k_a$ ) and was significantly different for the association constant among the tested 14-3-3 dimers (Table 1).

We have previously shown that single-Ser31 phosphorylation does not facilitate 14-3-3 binding (Kleppe *et al.* 2001), but the impact of double phosphorylation on Ser19 and Ser31 has not been investigated. Since TH did not show any particular preference in binding to different 14-3-3 dimers, we only investigated the binding between TH-pS19pS31 and 14-3-3 $\zeta$  (Table 1). The measurements were performed as for TH-pS19pS40 (Fig. 6b). Calculated affinity of 14-3-3 $\zeta$  for TH-pS19 was similar to that of TH-pS19pS31, indicating that like Ser40, Ser31 is not contributing substantially to the net affinity of binding in the TH:14-3-3 complex.

### Dephosphorylation of TH-pS19 complex with 14-3-3 alters the dissociation rate

We previously reported that injection of high phosphatase activity accelerated the dissociation of the 14-3-3 $\gamma$ :TH-pS19 complex on surface plasmon resonance (SPR) (Kleppe *et al.* 2014b). We repeated this experiment for 14-3-3 $\zeta$  and investigated how injection of different activities of pNP influenced the dissociation rate of the complex (Fig. 6c). We found increasing dissociation rate of TH-pS19 for pNP activities up to about 40 U/ $\mu$ L, whereas it seemed to level off at about 7.5-fold at pNP activities higher than 40 U/ $\mu$ L (Fig. 6d). The dissociation rate of TH-pS19:14-3-3 $\zeta$  was now independent of phosphatase concentration, suggesting that the remaining pSer19 was not accessible in the complex. We did a refit of the biacore data for TH-pS19 binding to 14-3-3 $\zeta$  using the two state model of protein complex (Table S1), but these parameters did not fit well with a simulated experiment with added phosphatase (not shown). More extensive studies

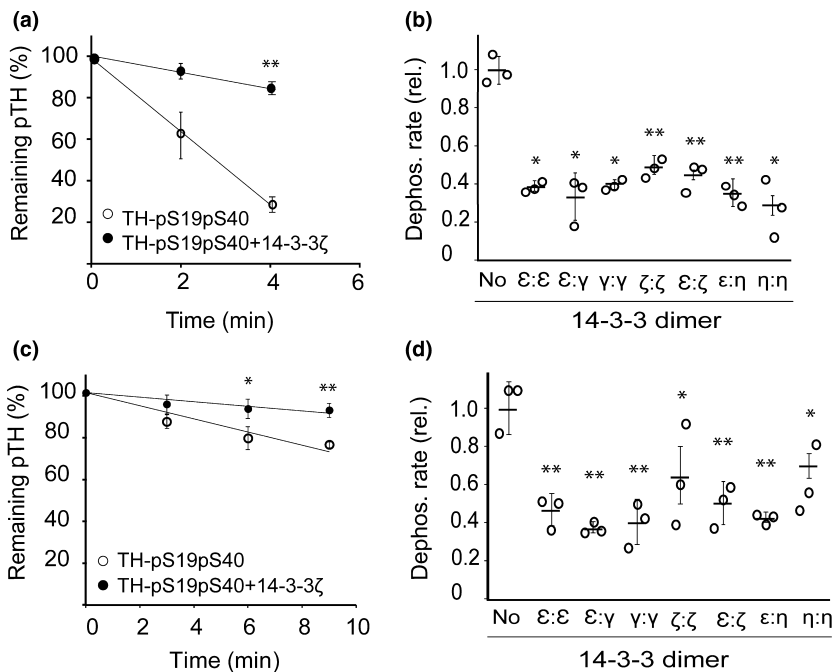


**Fig. 4** Dephosphorylation of TH at pSer40 in the presence or absence of different 14-3-3s. Dephosphorylation of pSer40 of the TH at Ser40 was measured in the presence (●) or absence (○) of different 14-3-3 dimers at 25°C. The TH-pS19pS40 (stoichiometry for Ser19 and Ser40 was  $1.0 \pm 0.01$  and  $1.0 \pm 0.04$ , respectively) was incubated with 10  $\mu$ M 14-3-3 as described in Methods. In (a and b) 70 U/mL pNP was used for dephosphorylation of TH-pS19pS40 (2  $\mu$ M). In (c and d) 1 mg/mL PC-12 cell lysate was used to dephosphorylate TH-pS19pS40 (1  $\mu$ M, c and 2  $\mu$ M, d). The error bars show the standard deviation from three different experiments. Statistical significance was evaluated using two tailed *t*-test and corrected for multiple comparisons using Holm-Bonferroni correction [ $n = 3$  (three different *in vitro* assay experiments)]; \*0.05 >  $p > 0.001$ ; \*\* $p < 0.001$ .

using complementary technologies will therefore be needed to provide a full kinetic characterization of the possible state transitions in the TH:14-3-3 complex.

#### Comparison of TH activity for different phosphorylated forms and the effect of 14-3-3

We tested the activity of TH in different phosphorylation states compared to the dephosphorylated form (Fig. 7). In general, the dual phosphorylated forms of TH were the most activated, with the strongest effect displayed by TH-pS19pS31 (Fig. 7). We also tested the effect of 14-3-3 $\gamma$  on the activity of the different TH-phosphovariants. The 14-3-3 $\gamma$  isoform was previously found to activate TH the most (Ghorbani *et al.* 2016). A moderate activation was consistently observed for all TH-pS19 forms, and while the most significant effect was shown by TH-pS19pS31, the total activation was the highest for TH-pS19pS40 in the presence of 14-3-3 $\gamma$ . As expected, 14-3-3 $\gamma$  had no effect on the activity of dephosphorylated TH.

#### Modeling of TH phosphorylation and effect of 14-3-3 binding

In the study by Bobrovskaya *et al.* they showed that anisomycin pre-treatment of bovine chromaffin cells, which leads to increased TH Ser19 phosphorylation only, stimulated the forskolin/cAMP/PKA-mediated Ser40 phosphorylation of TH (Bobrovskaya *et al.* 2004). We wanted to analyze more quantitatively how much of the observed cellular responses could be explained by the hierarchical effect of pSer19 on PKA mediated Ser40 phosphorylation reported *in vitro* (Bevilaqua *et al.* 2001; Toska *et al.* 2002),

i.e. up to 3-fold increase in the rate of PKA phosphorylation of the same subunit. Using simple kinetic modeling of TH Ser40 phosphorylation and dephosphorylation, we estimated the expected effect of a 3-fold hierarchical influence in the presence of the observed pSer19 levels, and compared these predictions to the observed effects (Fig. 8). We first tested a linear model (see supplemental text for details). This model estimated very little effects of the observed pSer19 stoichiometries at the favorable conditions for hierarchical phosphorylation modeled here (Fig. 8A,B). Still we wanted to test if a non-linear kinetics could explain the observed phosphorylation effects by hierarchical phosphorylation. Thus, high signal sensitivity, e.g. zero order ultrasensitivity (Goldbeter and Koshland 1984), can arise at conditions close to substrate saturation for kinase and phosphatase. We used Michaelis-Menten kinetics assuming first a total TH concentration in the cells 5-fold the  $K_m$  value for Ser40 kinase and phosphatase (e.g., PP2A and PKA). This level of substrate saturation could not explain the observed signaling responses by the 3-fold hierarchical effect only (Fig. 8a). However, at TH concentrations 18-fold higher than the  $K_m$  values, the model was found to fit the observed signaling response of forskolin and anisomycin by only considering the hierarchical interaction (Fig. 8a,c), without any inhibitory influence from catecholamines or 14-3-3 proteins.

We further performed modeling to investigate possible effects of 14-3-3 binding on the steady state phosphorylation status of target proteins (TPs) at sites that are only partially inaccessible in the complex. We have previously performed mathematical modeling to analyze the influence of 14-3-3 proteins on target protein phosphorylation. In that context,

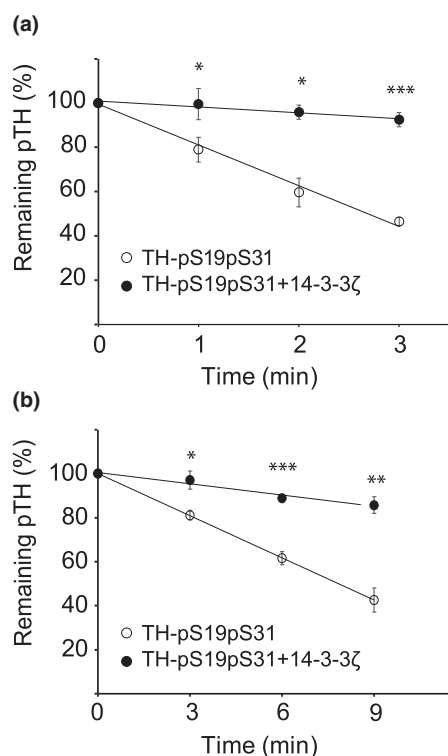


**Fig. 5** Effect of 14-3-3 $\zeta$  on dephosphorylation of pSer31. Dephosphorylation of phospho-Ser31 was measured in the absence (○) or presence (●) of 14-3-3 $\zeta$ . The TH-pS19pS31 (stoichiometry for Ser19 and Ser31 was  $1.0 \pm 0.01$  and  $0.90 \pm 0.02$ , respectively) was incubated with the 14-3-3 (10  $\mu$ M) and phosphatase as described in Methods. In (a) 50 U/mL pNP was used for dephosphorylation of TH-pS19pS31 (2  $\mu$ M), whereas in (b) 1 mg/mL PC-12 cell lysate was used for dephosphorylation of TH-pS19pS31 (1  $\mu$ M). The *p*-values were calculated by two tailed *t*-test ( $n = 3$  (three different *in vitro* assay experiments), average  $\pm$  SD); \**p* = 0.01; \*\**p* = 0.0006; \*\*\**p* <  $2.9 \times 10^{-5}$ .

the pSer19 (primary site, S1) and 14-3-3 binding to TH would correspond to the type of target protein where total Ser40 or Ser31 phosphorylation (secondary, but functional sites, S2) would be of interest (Kleppe *et al.* 2014a). The analysis performed then suggested no influence of 14-3-3 on the amplification of secondary site phosphorylation at conditions where little/no binding would happen in absence of primary site phosphorylation (similar  $K_d$ -values for TP-pS1 and TP-pS1pS2, such as observed for TH-pS19 versus TH-pS19pS40 or TH-pS19pS31). However, the previous modeling approach did not consider the possibility of phosphorylation or dephosphorylation in the protein complex. We therefore investigated how such partial accessibility would influence the effect of 14-3-3 proteins on target protein phosphorylation of the functional site (S2, Fig. 9a). Using the same modeling approach as previously, we investigated the conditions where phosphorylation and dephosphorylation kinetics were influenced differently by

the complex formation (Fig. 9b,c). Different access to the functional site in the complex could be caused by different ratio or exchange kinetics between “open” and “closed” states in the mono- and dual phosphorylated states or simply different steric accessibility for the kinase versus phosphatase. Thus, depending on which process is influenced more, such 14-3-3 complex formation can provide both positive (Fig. 9b) or negative (Fig. 9c) signaling cross-talk.

## Discussion

Multisite phosphorylation of proteins is a molecular mechanism that can generate switching behavior or ultrasensitive responses of cellular pathways (Ferrell *et al.* 2014; Nishi *et al.* 2015). However, the initiation of such behavior may rely on complex relationships. TH activity is under strict control in cells as catecholamines are reactive and their synthesis and degradation generates reactive oxygen species (Haavik *et al.* 1997; Delcambre *et al.* 2016). The catalytic activity of TH is strongly suppressed by active site binding of inhibitory catecholamines, which can be released upon Ser40 phosphorylation (Andersson *et al.* 1988; Daubner *et al.* 1992; Sura *et al.* 2004; Lehmann *et al.* 2006). In the nervous system, TH is also controlled by auto receptors that suppress Ser40 phosphorylation upon binding of released catecholamines, for example, dopamine in the striatum (Lindgren *et al.* 2001). The strict control of the Ser40 could suggest it might be targeted by multisite phosphorylation effector mechanisms, where particular combinations of signals or their temporal pattern is important to execute a proper response. The possible functional implication of multisite phosphorylation of TH was first reported as hierarchical phosphorylation, stimulating Ser40 phosphorylation via prior phosphorylation of Ser19 or Ser31 (Bevilaqua *et al.* 2001; Bobrovskaya *et al.* 2004; Lehmann *et al.* 2006). In this study, we provide new *in vitro* evidence supporting that phospho-site communication influence TH dephosphorylation, and that in the case of Ser19 phosphorylation, there is additional modulation of the phospho-site communication by 14-3-3 proteins.

The *in vitro* approach taken in this work has several advantages, such as the full control of phosphorylation status and the identity and binding stoichiometry of the 14-3-3 proteins present. It also allows us to study the cross-talk between different phosphorylated sites of TH and 14-3-3 protein binding without the possibility of interfering the cross-talk at the level of the upstream signaling pathways. In fact, several examples have been reported, such as between  $Ca^{2+}$  signaling and MAPK signaling (Griffiths and Marley 2001; Knowles *et al.* 2011), or PKA signaling (Luo *et al.* 2017), CDK5 and PKA signaling (Plattner *et al.* 2015). In addition, it is challenging to measure phosphorylation stoichiometry in cells and to control the influence from multiple 14-3-3 proteins. The results presented here show the

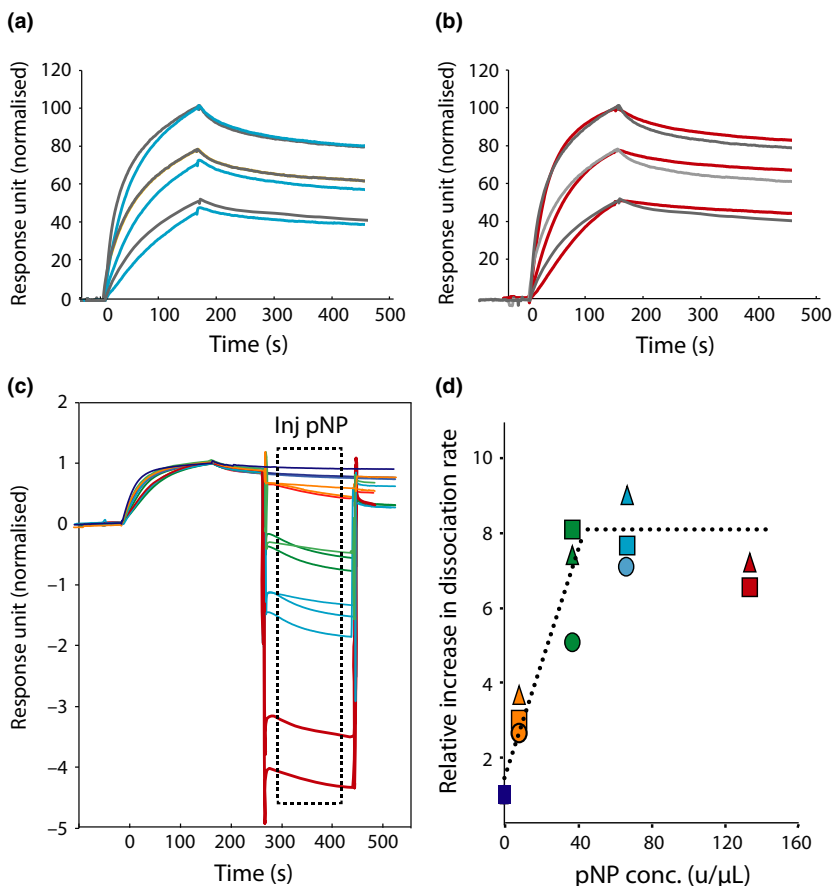


**Fig. 6** Binding of different TH phosphoforms to immobilized 14-3-3 $\zeta$ . Ser19, Ser40 and Ser31 were phosphorylated by PRAK, PKA, and CDK5, respectively. The association and dissociation kinetic for phosphorylated TH to 14-3-3 $\zeta$  was measured using surface plasmon resonance (SPR) (Methods). GST-14-3-3 $\zeta$  was immobilized to a CM5 chip (GE Healthcare) using a GST-immobilization kit (GE Healthcare) according to manufacturer's protocols. Sensograms were recorded at a flow rate of 30  $\mu$ L/min. The figure indicates the comparison between (a) injected (90  $\mu$ L) TH-pS19 (25, 50 and 100 nM, gray) and TH-pS19pS40 (25, 50, and 100 nM, blue). (b) TH-pS19 (25, 50 and 100 nM, gray) and TH-pS19pS31 (25, 50, and 100 nM, red). Sensograms were scaled for illustration of kinetics. (C and D) The panels show the increase in dissociation rate of TH-pS19:14-3-3 $\zeta$  complex that was measured after 2-3 repeated injections of different concentrations of pNP (5, 37, 67, 134 U/mL).

events that can potentially occur *in vivo*, given the right circumstances. The results, however, do not address complexities rising in a cellular setting from the simultaneous action of kinases, phosphatases, and 14-3-3 binding, as well as possible changes in protein localization as a result of this (Jorge-Finnigan *et al.* 2017; Kunzler *et al.* 2019).

The effect of pSer19 on CDK5 mediated Ser31 phosphorylation has not been reported previously. The lack of any such effect was reported for the Ser19 phospho-mimicking mutant TH-Ser19Glu, however, this could be because of the less charge density as the Ser40 phosphorylated Ser19Glu mutant showed more efficient Ser31 phosphorylation than the Ser40 phosphorylated wt TH (Kansy *et al.* 2004). Our results strengthen the hypothesis of a substrate conformational change underlying the mechanism of the hierarchical Ser19 effect. Thus, the positive multisite cross-talk reported so far has been observed using PKA mediated Ser40 phosphorylation, and could therefore be kinase specific. However, as PKA and CDK5 are kinases from different families, and both show increased phosphorylation efficiency in response to pSer19, it seems more likely to be caused by a conformational change in TH. In this scenario, the initial phosphorylation leads to an opening within the flexible N-terminal region, making Ser40 more available for the kinase,

which is also the proposed mechanism for the hierarchical effect on Ser40 by pSer19 and pSer31 (Bevilaqua *et al.* 2001). This mechanistic interpretation is consistent with several observations; the stronger effect of Ser19 on Ser31 (4.7-fold) than on the more distant site Ser40 (2-3-fold), as observed in this study; the stronger effect of Ser31 on Ser40 (9-fold) (Lehmann *et al.* 2006; Gordon *et al.* 2009); and the negative effect of catecholamines, which pulls the N-terminal region surrounding Ser40 closer to the active site (Wang *et al.* 2009b). The structure of the far N-terminal region and regulatory domain of TH is not yet resolved, however, recent measurements using small-angle X-ray scattering suggests a highly extended structure for the region where the phosphorylation sites are located (Bezem *et al.* 2016). As of yet, it is not known how phosphorylation on the different sites affects the conformation of the far N-terminal region, however, molecular dynamics simulations suggest that Ser19 phosphorylation reduces the flexibility of this region (Skjjevik *et al.* 2014).

TH phosphorylation at Ser19, Ser31, and Ser40 is well documented to be dynamically controlled by several different signaling pathways in cells and tissues (Haycock 1990; Dunkley *et al.* 2004), see (Dunkley and Dickson 2019) for a recent comprehensive review. Whereas Ser19 and Ser31

**Table 1** Binding kinetics for complex formation between 14-3-3 isoforms and multisite phosphorylated TH

14-3-3 protein	Site(s) phosphorylated in TH	$k_a$ ( $10^5 \text{ M}^{-1}\text{s}^{-1}$ ) [ $\chi^2$ of fit]	$k_d$ ( $10^{-3}\text{s}^{-1}$ ) [ $\chi^2$ of fit]	$K_d$ (nM)
ε:ε	pS19	2.6 ± 0.90	0.72 ± 0.10	2.8
	pS19 & pS40	3.0 ± 0.30 [0.0967]	0.83 ± 0.24 [0.0247]	2.8
γ:γ	pS19	3.1 ± 1.5	0.94 ± 0.10	3.0
	pS19 & pS40	1.6 ± 0.54 [0.587]	0.36 ± 0.06 [0.0178]	2.1
ζ:ζ*	pS19	1.9 ± 0.40	0.30 ± 0.08	1.6
	pS19 & pS40	2.1 ± 0.48 [0.092]	0.30 ± 0.03 [0.026]	1.4
	pS19 & pS31	1.6 ± 0.40 [0.115]	0.30 ± 0.1 [0.0319]	2.0
η:η	pS19	2.7 ± 0.80	0.44 ± 0.06	1.6
	pS19 & pS40	1.3 ± 0.47 [0.145]	0.20 ± 0.04 [0.0214]	1.5
β:β	pS19	2.2 ± 0.80	0.30 ± 0.02	1.4
	pS19 & pS40	2.8 ± 0.90 [0.0609]	0.42 ± 0.05 [0.0219]	1.5
ε:γ	pS19	2.0 ± 1.0	0.50 ± 0.07	2.5
	pS19 & pS40	2.6 ± 0.46 [0.367]	0.40 ± 0.05 [0.0219]	1.5
ε:ζ	pS19	1.7 ± 0.86	0.65 ± 0.07	3.8
	pS19 & pS40	2.1 ± 0.26 [0.157]	0.26 ± 0.04 [0.0228]	1.2
ε:η	pS19	2.9 ± 1.1	0.48 ± 0.04	1.7
	pS19 & pS40	1.3 ± 0.32 [0.275]	0.32 ± 0.02 [0.0216]	2.5
ε:β	pS19	2.0 ± 1.0	0.50 ± 0.10	2.5
	pS19 & pS40	1.1 ± 0.30 [0.55]	0.30 ± 0.02 [0.012]	2.5

Using SPR (Methods) we fitted the association and dissociation rate constants for binding of different 14-3-3 dimers to TH phosphorylated on Ser19 (using PRAK, 0.4 mol phosphate/mol TH subunits), Ser40 (using PKA, 0.7 mol phosphate/mol TH subunits) and on Ser31 (using CDK5, 0.6 mol Phosphate/mol TH subunits). Two separate immobilizations of 14-3-3 were used and at least three different concentrations of TH were injected for each of them. Values of rate constants are shown ± SEM. Single factor ANOVA of all  $k_a$  and  $k_d$ -values showed that only the  $k_a$  constants differed significantly between the 14-3-3 dimer types ( $p = 7.0 \cdot 10^{-6}$ ). The data for TH-pS19 is extracted from our previous findings (Ghorbani *et al.* 2016) and is presented here for comparison, except for 14-3-3:ζ where all sites were fitted from new data (\*).

have been found at substantial phosphorylation stoichiometries in cells (0.05–0.2 and 0.08) (Haycock *et al.* 1998; Salvatore *et al.* 2001; Bobrovskaya *et al.* 2004) and brain tissue (0.1–0.27 and 0.05–0.3) (Salvatore *et al.* 2000; Salvatore and Pruetz 2012), the reported phosphorylation stoichiometry of TH-pS40 is generally very low (0.02–0.05) (Haycock *et al.* 1998; Bobrovskaya *et al.* 2004; Salvatore

and Pruetz 2012). It is still largely unknown to what degree TH is multi-phosphorylated *in vivo*, that is, phosphorylated at several sites simultaneously in the same subunit or in the same tetramer.

The observed stimulatory effect of Ser19 phosphorylation signaling pathways on TH phosphorylation at Ser40 in cells – for example, by PKA – has been ascribed to the hierarchical phosphorylation effect discovered *in vitro*. Using kinetic modeling we tested the requirements for this to occur, finding that 18-fold higher TH concentration than the  $K_m$  value for both kinase and phosphatase was needed. The  $K_m$  values for kinases and phosphatases of TH are not well characterized. However, the  $K_m$  value for PKA has been estimated to about 5 μM for TH (Almås *et al.* 2000) and probably higher for PP2A (Bevilaqua *et al.* 2003), suggesting that > 90 μM TH is needed to obtain the observed increase in phosphorylation by hierarchical effects only.

Still, several conditions in the cell may negatively influence the hierarchical interaction between Ser19 and Ser40. Thus, catecholamine binding seems to disturb the hierarchical phosphorylation (Lehmann *et al.* 2006) and a 30 min preincubation with anisomycin would expectedly provide ample opportunity for 14-3-3 protein binding, presumably resulting in reduction of the hierarchical interaction as reported here. In light of these inhibitory mechanisms, the 14-3-3 mediated inhibition of dephosphorylation reported here may compensate for the negative effects on phosphorylation that can occur in cells and may be an additional mechanism by which phospho-site synergies may arise in cells.

Cellular labeling studies have suggested more rapid dephosphorylation of Ser40, compared to Ser19 and Ser31 (Leal *et al.* 2002). Our findings suggest that dephosphorylation kinetics of TH is complex. For singly phosphorylated TH, TH-pS31 was clearly dephosphorylated more rapidly than TH-pS40 *in vitro*. In the presence of pSer19, this was less clear and binding of 14-3-3 proteins inhibited pSer31 dephosphorylation more strongly than pSer40. These mechanisms as well as interaction with other proteins (Jorge-Finnigan *et al.* 2017) or localization of TH to specific cellular compartments, such as mitochondria (Wang *et al.* 2009a), Golgi and synaptic vesicles (Jorge-Finnigan *et al.* 2017) may underlie the apparent controversy. It is therefore likely that TH phosphorylation at different sites show different dynamics and degree of interaction between the sites at different cellular localizations, in particular between terminal and somatodendritic compartments, as reported (Salvatore and Pruetz 2012).

The effect of multisite phosphorylation on TH dephosphorylation has not been noted previously. Our results showed that the presence of pSer19 partially protects pSer31 from dephosphorylation, and less so for pSer40. It has been reported that phosphorylation of Ser19 possibly decreases dephosphorylation of Ser31 and Ser40 (Gonçalves *et al.*

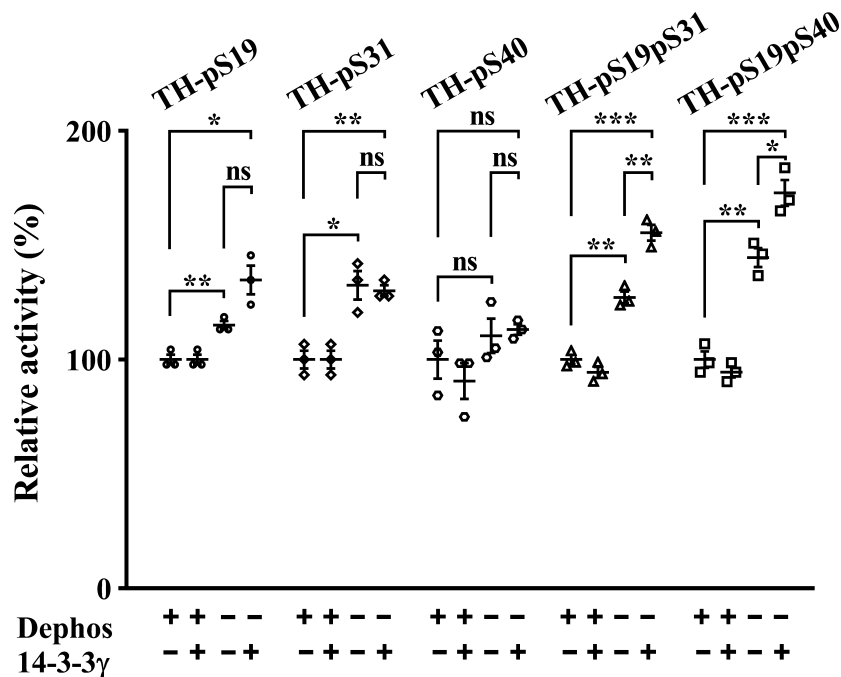


**Fig. 7** Relative enzyme activity of hTH1 phospho-variants in the presence and absence of 14-3-3 $\gamma$ . Single and double phosphorylated hTH1 samples were subjected to activity measurements in the presence or absence of 14-3-3 $\gamma$  (60  $\mu$ g/mL). Controls for all phospho-variants were created through dephosphorylation with SAP (1U, 25°C, in 10 min reactions). Phosphorylation at either site yielded higher enzymatic activity, however, only the double phosphorylated variants showed significant activation by 14-3-3 $\gamma$ . Although the effect on the TH-pS19 (○) variant was also notable, it was not determined to be significant

1997) in cells and our *in vitro* findings clearly supports this. These results are intriguing as they suggest less access to pSer31 for phosphatases, opposite to the case for TH-pS19. Possibly, the dual phosphorylated TH adapts a closed conformation as opposed to the singly phosphorylated protein.

An interesting finding in this study was the influence of 14-3-3 protein binding on both phosphorylation and dephosphorylation. This was more evident for Ser31, possibly as it is closer to Ser19. Binding of 14-3-3 to some target proteins is known to depend on target phosphorylation on two sites, where phosphorylation on one site contributes the most to the binding affinity and the other site acts to further strengthen the 14-3-3 binding (Mils *et al.* 2000; Mackintosh 2004). As the binding kinetics and affinity of TH to 14-3-3 was not changed much by Ser40 or Ser31 phosphorylation, we could presume that these phosphoserines do not dock into either of the two phospho-recognition sites of the 14-3-3 dimer. Using NMR on Ser19 and/or Ser40 phosphorylated forms of the N-terminal peptide (50 aa) of TH evidence was found for a pSer19 & pSer40 interaction with 14-3-3 $\zeta$  (Hritz *et al.* 2014). However, 14-3-3 with two peptides bound via the pSer19

( $p = 0.07$ ). Our main finding was that while alone, TH-pS31 (◇) and TH-pS40 (hexagons) phospho-variants showed no activation by 14-3-3 $\gamma$ , however, double phosphorylated TH-pS19pS31 (Δ) as well as TH-pS19pS40 (□) markedly outperformed TH-pS19 both in the presence and absence of 14-3-3 $\gamma$ . This indicates that secondary phosphorylation may have facilitatory effect on TH activity. All P values were calculated using two-tailed Welch's *t*-test in GraphPad Prism 7.0 ( $n = 3$  (three different *in vitro* assay experiments), average  $\pm$  SEM); \*\*\* $p < 0.001$ ; \*\* $0.001 < p < 0.01$ ; \* $0.01 < p < 0.05$ ; not significant for  $0.05 < p$ .

residue was more prevalent and high concentrations of peptide were used compared to our SPR experiments. Still, although peptides are more flexible, it cannot be excluded that 14-3-3 dimers can bind to both pSer19 and pSer40 in the case where the two neighboring Ser19 residues are not both phosphorylated. The structure of the TH:14-3-3 protein complex is not known, however, the complex between 14-3-3 $\zeta$  and the N-terminal TH peptide has been determined, showing an extended conformation of the region surrounding pSer19 (Skjervek *et al.* 2014).

We have determined a maximal 1:1 subunit stoichiometry between TH-pS19 and 14-3-3 $\gamma$  or TH-pS19pS40 and 14-3-3 $\gamma$  (Kleppe *et al.* 2014b). Furthermore, we observed the same binding kinetics for TH-pS19 to 14-3-3 $\gamma$  at different substoichiometric phospho-states as well as the same mono-exponential dephosphorylation kinetics, about fourfold higher than the dissociation rate constant of the complex in absence of phosphatase (Kleppe *et al.* 2014b). This fits with our observations here, that increasing phosphatase concentrations give increasing dissociation of the TH:14-3-3 complex up to a maximal rate, about sevenfold higher for 14-3-3 $\zeta$ .

These observations could suggest that two pSer19 residues from neighboring subunits interact with 14-3-3 proteins in a non-static complex. In this case, different conformational states must exist for the complex i.e. more closed and more open states. The ability of R18 to accelerate the dissociation of TH-pS19 from 14-3-3 proteins in SPR experiments, is consistent with such a model. Hence, in the closed state we propose that pSer19 from two neighboring N-terminal domains may bind in an anti-parallel conformation to their own phospho-recognition site in each subunit of the 14-3-3 dimer, unavailable for dephosphorylation (Fig. 10). In the more open and relaxed complex state, only one of the pSer19 coordinates to the phospho-recognition site of 14-3-3,

whereas the other pSer19 is more free to move outside the binding groove of 14-3-3, making it accessible to phosphatases, or kinases in the non-phospho state (Fig. 10). This fits with previous observations that PRAK phosphorylation of hTH1 was inhibited by the yeast 14-3-3 protein, BMH1, but not the more rapid and promiscuous phosphorylation by MAPKAP-K2 (Kleppe *et al.* 2002). In a more recent study we did not observe this effect using 14-3-3 $\gamma$  on PRAK phosphorylation of hTH1 (Kleppe *et al.* 2014b). These conflicting observations could be related to experimental conditions and differences in PRAK phosphorylation kinetics of the tetramer compared to the possibly competing binding kinetics of different 14-3-3 proteins. Thus, for PRAK or other kinases that phosphorylate TH, we do not know the degree of random versus preferential phosphorylation of neighboring subunits in the TH tetramer at different experimental conditions, PRAK concentrations and preparations. We expect further that there are differences between the human TH isoforms in the degree of multisite phosphorylation cross-talk, effects of 14-3-3 protein binding and the kinetics of state-transitions in the TH:14-3-3 complex. Although not very abundantly expressed, the longer isoforms, hTH3 and hTH4, are expected to show differences as the inserted amino acids leads to a longer distance between the Ser19- and the “Ser40” sites.

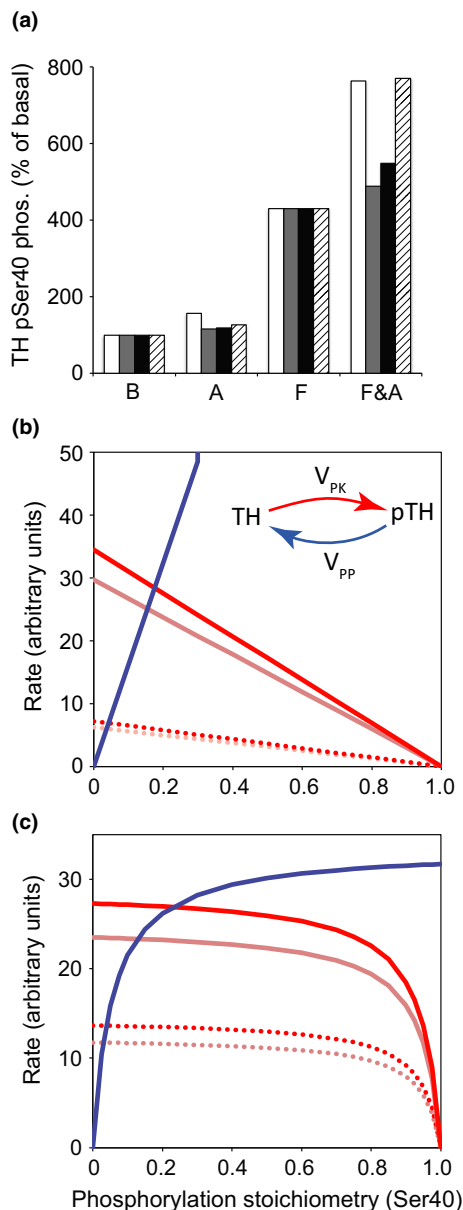


**Fig. 8** Mathematical modeling of hierarchical phosphorylation between Ser19 and Ser40. (a) Based on experimentally observed phosphorylation stoichiometries (Boborovskaya *et al.* 2004) (white bars, shown as % of basal), we estimated the effect of pSer19 (stoichiometry at basal and during anisomycin stimulation, 0.12 and 0.22, respectively) on Ser40 phosphorylation. The modeling was performed using linear kinetics (b) (a, grey bars) or Michaelis–Menten (MM) kinetics (c) (a, black and striped bars) for kinase and phosphatase. A threefold stimulation of the rate of PKA phosphorylation ( $k_{PK}$  or  $V_{max}$ ) in the presence of pSer19 was included and for the MM model, a concentration of total [TH] 5-fold the  $K_m$ -value (black bars) or 18-fold (striped bars) was included. (b) and (c) show the rate of dephosphorylation (blue) and phosphorylation (red curves) at different Ser40 stoichiometries. Steady state values of TH Ser40 phosphorylation stoichiometry are where the two rates are equal. The rate of phosphorylation is shown at basal (dotted) or forskolin stimulated (full lines) in absence (light red) or presence (red) of anisomycin. For (c) the situation of 18-fold higher  $[TH]_{tot}$  than the  $K_m$  value is shown. This means that the kinetics operates close to saturation, that is, at conditions where the phosphorylation response is very sensitive to changes in the phosphorylation kinetics. The models were adjusted to fit the basal and forskolin (PKA) stimulated conditions observed experimentally and then used to estimate the phosphorylation stoichiometry at Ser40 (shown in % of basal (0.03)), at the given observed Ser19 phosphorylation stoichiometry, as an effect of a threefold hierarchical intra-subunit interaction of pSer19 with Ser40, only. No negative effect on the hierarchical interaction was included from possible catecholamine or 14-3-3 binding. See supplementary text for details on the modeling.

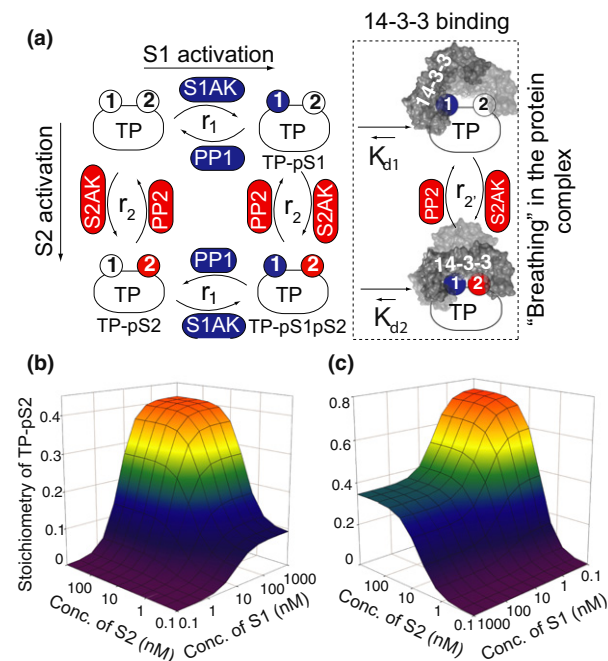


**Fig. 9** Altered accessibility to phosphorylation sites in 14-3-3 protein complexes can give rise to both positive or negative signaling cross-talk. (a) Shows the kinetic scheme for a 14-3-3 target protein (TP) with one phosphorylation site (site 1, targeted by a S1 signaling pathway), which is necessary for complex formation. A different phosphorylation site of TP (site 2, targeted by a S2-signaling pathway), which is important for regulation of the protein, but is not contributing to the affinity of the complex, is included. Access to site 2 is influenced by binding of 14-3-3. For the situation where dual phosphorylation do not affect the affinity of TP to 14-3-3;  $K_{d1} = K_{d2}$ , no synergy between the two pathways is induced by 14-3-3 (Kleppe *et al.* 2014a). Differing accessibility to site 2 (important for regulation of the physiological function of the target protein) by kinases or phosphatases in the TP:14-3-3 complex can act to induce stimulatory or inhibitory interactions of the S1-pathway with site 2 phosphorylation if the ratio of the phosphatase and kinase rate constants is decreased or increased in the complex ( $r_2' = k_{PP2}/k_{PK2}$ ) relative to that of free TP ( $r_2 = k_{PP2}/k_{PK2}$ ), respectively. Here we used parameters;  $K_{d1} = K_{d2} = 5.0$  nM, and rate constants (all  $s^{-1}$ ) of  $k_{PK1} = 1.0$ ,  $k_{PP1} = 5.0$  ( $r_1 = 5.0$ ) for site 1 (gate-keeper site, necessary for 14-3-3 binding). In panel (b) is shown the case of signal amplification. Parameters; free TP;  $k_{PK2} = 1.0$ ,  $k_{PP2} = 10$ , in complex with 14-3-3;  $k_{PK2}' = 1.0$ ,  $k_{PP2}' = 1.0$ . In panel (c) is shown the case with 14-3-3-mediated antagonistic signal interaction. Parameters used were: For free TP;  $k_{PK2} = 3.0$ ,  $k_{PP2} = 1.0$  ( $r_2 = 3.0$ ), in complex with 14-3-3;  $k_{PK2}' = 0.3$ ,  $k_{PP2}' = 1.0$  ( $r_2' = 0.3$ ).

There are several studies that point to the involvement of 14-3-3 proteins in neuropsychiatric disorders and neurodegenerative diseases such as Parkinson's disease (Ramshaw *et al.* 2013; Jacobsen *et al.* 2015; Lavalley *et al.* 2016; Kelly *et al.* 2019). Mechanistically, this is expected to occur through their interaction with other protein targets than TH, but that are in many cases expressed in the same cell types,

such as the dopamine transporter (Ramshaw *et al.* 2013) and the Leucine-rich repeat kinase 2 (Lavalley *et al.* 2016). 14-3-3 proteins have been found to regulate the phosphorylation state of other target proteins as well. In a modeling study we investigated quantitative aspects of 14-3-3 proteins interacting with multisite phosphorylated target proteins (Kleppe *et al.* 2014a). Different conditions were derived for 14-3-3 mediated positive cross-talk between signaling pathways targeting different sites on target proteins. One such target protein where 14-3-3 proteins are reported to affect its phosphorylation status is the apoptotic protein Bcl-2-associated death promoter (BAD). Regulation of BAD involves a high level of cross-talk among its phosphorylated sites. Chiang *et al.* in their study showed that 14-3-3 protects all three phosphorylated serine residues of BAD (Ser112, Ser136, Ser155) from the action of phosphatases, while only phospho-Ser136 is the major 14-3-3 recruitment site and phospho-Ser112 increases the stability of BAD:14-3-3 complex, but is not necessary for the complex formation. They showed that phosphorylation at Ser112 inhibits Ser136 from dephosphorylation while dephosphorylation of phospho-Ser112 renders phospho-Ser136 accessible to phosphatases by destabilizing the interaction between 14-3-3 and BAD, facilitating the phosphatase activity on phospho-Ser136. PP2A or PP2A-like phosphatases were shown to specifically target Ser112, while dephosphorylation of Ser136 and Ser155 were not limited to one specific phosphatase family. Access to this site is completely prevented in presence of 14-3-3 protein (Chiang *et al.* 2003; Chiang *et al.* 2003). The results from BAD and from this study could be useful to understand other multisite phosphorylated 14-3-3 binding proteins such as Tau.

We propose a model where 14-3-3 proteins actively participate to shape the phosphorylation-mediated regulation of their target proteins, both as secondary effector proteins and as direct modulators of the phosphorylation and dephosphorylation kinetics. For TH, we provide additional evidence underlying the role of Ser19 as a modulatory site for TH multisite phosphorylation of the functional sites Ser31 and Ser40. Both at the level of direct conformational alterations affecting kinase and phosphatase binding and action as well as 14-3-3 binding, which both alter the kinetics of phosphorylation and dephosphorylation. We speculate if this can have implications for the coordinated timing of neuronal signaling events that target TH by phosphorylation, whether they occur sequentially, but not too delayed to exploit the hierarchical effects of phosphorylation prior to 14-3-3 binding. And with respect to dephosphorylation, if the activation of the signaling pathway is sustained for sufficient time to allow 14-3-3 proteins to bind and inhibit dephosphorylation. These questions will have to be tested at experimental settings that allow monitoring of TH phosphorylation at conditions where stimulation of different signaling pathways is dynamically controlled.

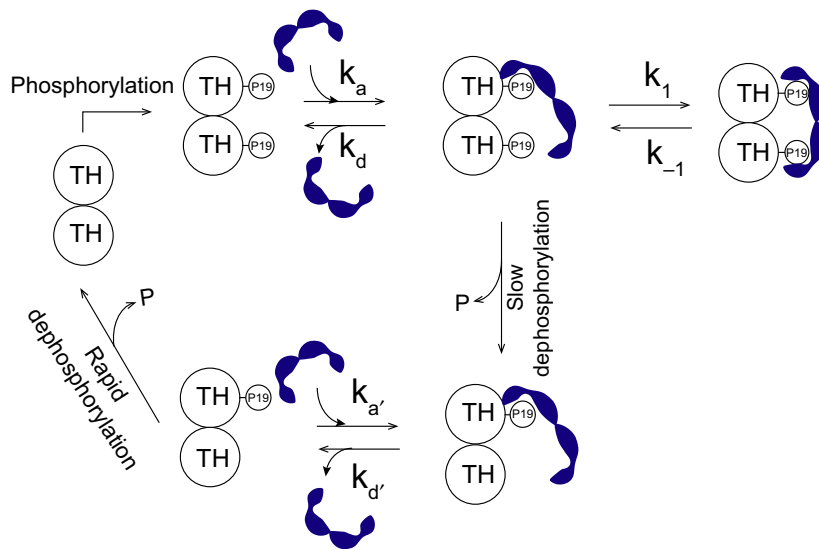


**Fig. 10** Two state model of the TH-pS19:14-3-3 complex. Based on structural data on TH (Bezern et al. 2016) and observed maximal stoichiometry of two 14-3-3(ζ) dimers binding to the TH(pS19 & pS19pS40) tetramer (Kleppe et al. 2014b), we propose a cartoon model of the protein complex and its kinetic states. TH is a dimer of dimers, where each dimer contributes with an N-terminal regulatory domain residing two and two at opposite sides of the plane containing the four catalytic subunits. We have therefore only illustrated the kinetics and available states in the complex for the two TH N-terminals residing on the same side. Assuming independent binding of the two

14-3-3 proteins to tetrameric TH, a similar kinetic scheme will apply to the other two N-terminals of TH in the same tetramer. We propose that the phospho-TH:14-3-3 complex can reside in two states; a closed state (far right), where two pSer19 are hidden in the 14-3-3 binding groove, inaccessible to phosphatases, where for at least one of the two N-terminals, the pSer19 is docked in the phospho-recognition site of 14-3-3; an open state (middle) where only one pSer19 is properly docked to the 14-3-3 phospho-recognition site and the other pSer19 being accessible for dephosphorylation and not contributing much to the binding.

The observation that the TH:14-3-3 complex could be dynamic and may exist transiently in a more open conformation, has implications for the possible drug targeting of the complex. The proposed open conformation is the only state that could be accessible for inhibitors or stabilizers that target the binding groove of 14-3-3 proteins. The existence of such a state would therefore open up for targeting the complex itself, rather than the free 14-3-3 proteins, which would be expected to have much larger negative consequences. Furthermore, the kinetic observations of the TH:14-3-3 complex may be relevant for other 14-3-3 target proteins as well.

## Acknowledgments and conflict of interest disclosure

The authors thank professor Aurora Martinez and Dr Ana Jorge-Finnigan for their valuable advice and critical reading of the manuscript. This work was supported by the University of Bergen, Stiftelsen Kristian Gerhard Jebsen (SKGJ-MED-002), NevSom (grant number 51379) and the Western Norwegian Health Authorities (Helse-Vest). The authors declare no conflict of interest.

All experiments were conducted in compliance with the ARRIVE guidelines.

## Supporting information

Additional supporting information may be found online in the Supporting Information section at the end of the article.

**Figure S1.** SDS-page and gel filtration analysis of purification of TH.

**Figure S2.** SDS-page and gel filtration analysis of purification of 14-3-3 homo- and heterodimers.

**Figure S3.** Western blot analysis of PC12 lysate.

**Figure S4.** Dephosphorylation of TH at Ser40 in the presence of different 14-3-3s.

**Table S1.** Fitting of TH-pS19 binding to 14-3-3ζ by a two state complex model.

## References

- Albert K. A., Helmer-Matyjek E., Nairn A. C., Müller T., Haycock J. W., Greene L. A., Goldstein M. and Greengard P. (1984) Calcium/phospholipid-dependent protein kinase (protein kinase C) phosphorylates and activates tyrosine hydroxylase. *Proc. Natl Acad. Sci. USA* **81**, 7713–7717.
- Almås B., Bourdelles B., Flatmark T., Mallet J. and Haavik J. (1992) Regulation of recombinant human tyrosine hydroxylase isozymes by catecholamine binding and phosphorylation. *Eur. J. Biochem.* **209**, 249–255.

- Almås B., Toska K., Teigen K., Groehn V., Pfeleiderer W., Martinez A., Flatmark T. and Haavik J. (2000) A kinetic and conformational study on the interaction of tetrahydropteridines with tyrosine hydroxylase. *Biochemistry* **39**, 13676–13686.
- Andersson K., Cox D., Que L., Flatmark T. and Haavik J. (1988) Resonance Raman studies on the blue-green-colored bovine adrenal tyrosine 3-monoxygenase (tyrosine hydroxylase). Evidence that the feedback inhibitors adrenaline and noradrenaline are coordinated to iron. *J. Biol. Chem.* **263**, 18621–18626.
- Bevilaqua L. R., Graham M. E., Dunkley P. R., Nagy-Felsobuki E. I. and Dickson P. W. (2001) Phosphorylation of Ser19 alters the conformation of tyrosine hydroxylase to increase the rate of phosphorylation of Ser40. *J. Biol. Chem.* **276**, 40411–40416.
- Bevilaqua L. R., Cammarota M., Dickson P. W., Sim A. T. and Dunkley P. R. (2003) Role of protein phosphatase 2C from bovine adrenal chromaffin cells in the dephosphorylation of phospho-serine 40 tyrosine hydroxylase. *J. Neurochem.* **85**, 1368–1373.
- Bezem M. T., Baumann A., Skjærven L., Meyer R., Kursula P., Martinez A. and Flydal M. I. (2016) Stable preparations of tyrosine hydroxylase provide the solution structure of the full-length enzyme. *Sci. Rep.* **6**, 30390.
- Bobrovskaya L., Dunkley P. R. and Dickson P. W. (2004) Phosphorylation of Ser19 increases both Ser40 phosphorylation and enzyme activity of tyrosine hydroxylase in intact cells. *J. Neurochem.* **90**, 857–864.
- Campbell D. G., Hardie D. and Vulliet P. (1986) Identification of four phosphorylation sites in the N-terminal region of tyrosine hydroxylase. *J. Biol. Chem.* **261**, 10489–10492.
- Chiang C.-W., Kanies C., Kim K. W., Fang W. B., Parkhurst C., Xie M., Henry T. and Yang E. (2003) Protein phosphatase 2A dephosphorylation of phosphoserine 112 plays the gatekeeper role for BAD-mediated apoptosis. *Mol. Cell. Biol.* **23**, 6350–6362.
- Daubner S. C., Lauriano C., Haycock J. W. and Fitzpatrick P. F. (1992) Site-directed mutagenesis of serine 40 of rat tyrosine hydroxylase. Effects of dopamine and cAMP-dependent phosphorylation on enzyme activity. *J. Biol. Chem.* **267**, 12639–12646.
- Daubner S. C., Le T. and Wang S. (2011) Tyrosine hydroxylase and regulation of dopamine synthesis. *Arch. Biochem. Biophys.* **508**, 1–12.
- Delcambre S., Nonnenmacher Y. and Hiller K. (2016) Dopamine metabolism and reactive oxygen species production, in *Mitochondrial Mechanisms of Degeneration and Repair in Parkinson's Disease* (Buhlman L. M., ed), pp. 25–47. Springer.
- Dunkley P. R. and Dickson P. W. (2019) Tyrosine hydroxylase phosphorylation in vivo. *J. Neurochem.* **149**, 706–728.
- Dunkley P. R., Bobrovskaya L., Graham M. E., Nagy-Felsobuki E. I. and Dickson P. W. (2004) Tyrosine hydroxylase phosphorylation: regulation and consequences. *J. Neurochem.* **91**, 1025–1043.
- Ferrell J. E. and Ha S. H. (2014) Ultrasensitivity part II: multisite phosphorylation, stoichiometric inhibitors, and positive feedback. *Trends Biochem. Sci.* **39**, 556–569.
- Fossbakk A., Kleppe R., Knappskog P. M., Martinez A. and Haavik J. (2014) Functional studies of tyrosine hydroxylase missense variants reveal distinct patterns of molecular defects in Dopamine-responsive dystonia. *Hum. Mutat.* **35**, 880–90.
- Fu H., Subramanian R. R. and Masters S. C. (2000) 14-3-3 proteins: structure, function, and regulation. *Sci. Signal.* **40**, 617.
- Funakoshi H., Okuno S. and Fujisawa H. (1991) Different effects on activity caused by phosphorylation of tyrosine hydroxylase at serine 40 by three multifunctional protein kinases. *J. Biol. Chem.* **266**, 15614–15620.
- Ghorbani S., Fossbakk A., Jorge-Finnigan A., Flydal M. I., Haavik J. and Kleppe R. (2016) Regulation of tyrosine hydroxylase is preserved across different homo- and heterodimeric 14-3-3 proteins. *Amino Acids* **48**, 1221–1229.
- Goldbeter A. and Koshland D. E. (1984) Ultrasensitivity in biochemical systems controlled by covalent modification. Interplay between zero-order and multistep effects. *J. Biol. Chem.* **259**, 14441–7.
- Gonçalves C. A., Hall A., Sim A. T., Bunn S. J., Marley P. D., Cheah T. B. and Dunkley P. R. (1997) Tyrosine hydroxylase phosphorylation in digitonin-permeabilized bovine adrenal chromaffin cells: The effect of protein kinase and phosphatase inhibitors on Ser19 and Ser40 phosphorylation. *J. Neurochem.* **69**, 2387–2396.
- Gordon S. L., Bobrovskaya L., Dunkley P. R. and Dickson P. W. (2009) Differential regulation of human tyrosine hydroxylase isoforms 1 and 2 in situ: isoform 2 is not phosphorylated at Ser35. *Biochim. Biophys. Acta* **1793**, 1860–1867.
- Griffiths J. and Marley P. D. (2001) Ca<sup>2+</sup>-dependent activation of tyrosine hydroxylase involves MEK1. *NeuroReport* **12**, 2679–2683.
- Haavik J., Schelling D. L., Campbell D. G., Andersson K. K., Flatmark T. and Cohen P. (1989) Identification of protein phosphatase 2A as the major tyrosine hydroxylase phosphatase in adrenal medulla and corpus striatum: evidence from the effects of okadaic acid. *FEBS Lett.* **251**, 36–42.
- Haavik J., Almås B. and Flatmark T. (1997) Generation of reactive oxygen species by tyrosine hydroxylase: a possible contribution to the degeneration of dopaminergic neurons? *J. Neurochem.* **68**, 328–332.
- Halskau Ø., Ying M., Baumann A., Kleppe R., Rodriguez-Larrea D., Almås B., Haavik J. and Martinez A. (2009) Three-way interaction between 14-3-3 proteins, the N-terminal region of tyrosine hydroxylase, and negatively charged membranes. *J. Biol. Chem.* **284**, 32758–32769.
- Haycock J. W. (1990) Phosphorylation of tyrosine-hydroxylase in situ at serine-8, serine-19, serine-31, and serine-40. *J. Biol. Chem.* **265**, 11682–11691.
- Haycock J. W., Ahn N. G., Cobb M. H. and Krebs E. G. (1992) ERK1 and ERK2, two microtubule-associated protein 2 kinases, mediate the phosphorylation of tyrosine hydroxylase at serine-31 in situ. *Proc. Natl Acad. Sci. USA* **89**, 2365–2369.
- Haycock J., Lew J., Garcia-Espana A., Lee K., Harada K., Meller E. and Goldstein M. (1998) Role of serine-19 phosphorylation in regulating tyrosine hydroxylase studied with site- and phosphospecific antibodies and site-directed mutagenesis. *J. Neurochem.* **71**, 1670–1675.
- Hoops S., Sahle S., Gauges R., Lee C., Pahle J., Simus N., Singhal M., Xu L., Mendes P. and Kummer U. (2006) COPASI: a Complex Pathway Simulator. *Bioinformatics* **22**, 3067–3074.
- Hritz J., Byeon I.-J. L., Krzysiak T., Martinez A., Sklenar V. and Gronenborn A. M. (2014) Dissection of binding between a phosphorylated tyrosine hydroxylase peptide and 14-3-3 zeta: a complex story elucidated by NMR. *Biophys. J.* **107**, 2185–2194.
- Itagaki C., Isobe T., Taoka M., Natsume T., Nomura N., Horigome T. and Omata S. (1999) Stimulus-coupled interaction of tyrosine hydroxylase with 14-3-3 proteins. *Biochemistry* **38**, 15673–15680.
- Jacobsen K. K., Kleppe R., Johansson S., Zayats T. and Haavik J. (2015) Epistatic and gene wide effects in YWHA and aromatic amino hydroxylase genes across ADHD and other common neuropsychiatric disorders: Association with YWHA. *Am. J. Med. Genet. B Neuropsychiatr. Genet.* **168**, 423–432.
- Jorge-Finnigan A., Kleppe R., Jung-KC K., Ying M., Marie M., Rios-Mondragon I., Salvatore M. F., Saraste J. and Martinez A. (2017) Phosphorylation at serine 31 targets tyrosine hydroxylase to vesicles for transport along microtubules. *J. Biol. Chem.* **292**, 14092–14107.
- Kansy J. W., Daubner S. C., Nishi A., Sotogaku N., Lloyd M. D., Nguyen C. and Lu L. (2004) Identification of tyrosine hydroxylase as a physiological substrate for Cdk5. *J. Neurochem.* **91**, 374–84.

- Kelly J., Moyeed R., Carroll C., Albani D. and Li X. (2019) Gene expression meta-analysis of Parkinson's disease and its relationship with Alzheimer's disease. *Mol. Brain*. **12**, 16.
- Kleppe R., Toska K. and Haavik J. (2001) Interaction of phosphorylated tyrosine hydroxylase with 14-3-3 proteins: evidence for a phosphoserine 40-dependent association. *J. Neurochem.* **77**, 1097–1107.
- Kleppe R., Toska K. and Haavik J. (2002) Interaction of Phosphorylated Tyrosine Hydroxylase with 14-3-3 Proteins: Effects on Phosphorylation Kinetics, in *Chemistry and Biology of Pteridines and Folates* (Milstien S., Kapatos G., Levine R. A., Shane B. eds), pp. 85–89. Springer, Boston.
- Kleppe R., Ghorbani S., Martinez A. and Haavik J. (2014a) Modelling cellular signal communication mediated by phosphorylation dependent interaction with 14-3-3 proteins. *FEBS lett.* **588**, 92–98.
- Kleppe R., Rosati S., Jorge-Finnigan A., Alvira S., Ghorbani S., Haavik J., Valpusta J. M., Heck A. J. and Martinez A. (2014b) Phosphorylation dependence and stoichiometry of the complex formed by tyrosine hydroxylase and 14-3-3 $\gamma$ . *Mol. Cell. Proteom.* **13**(8), 2017–2030.
- Knowles P., Douglas S. and Bunn S. (2011) Nicotinic stimulation of catecholamine synthesis and tyrosine hydroxylase phosphorylation in cervine adrenal medullary chromaffin cells. *J. Neuroendocrinol.* **23**, 224–231.
- Kopperud R., Christensen A. E., Kjarland E., Viste K., Kleivdal H. and Døskeland S. O. (2002) Formation of inactive cAMP-saturated holoenzyme of cAMP-dependent protein kinase under physiological conditions. *J. Biol. Chem.* **277**, 13443–8.
- Kunzler A., Garcia Sobrinho P., Smith T., Gelain D. P., Moreira J. C. F., Dunkley P. R. and Dickson P. W. (2019) Subcellular distribution of human tyrosine hydroxylase isoforms 1 and 4 in SH-SY5Y cells. *J. Cell. Biochem.* [Epub ahead of print] <https://doi.org/10.1002/jcb.29279>.
- Lavalley N. J., Slone S. R., Ding H., West A. B. and Yacoubian T. A. (2016) 14-3-3 Proteins regulate mutant LRRK2 kinase activity and neurite shortening. *Hum Mol Genet.* **25**, 109–122.
- Leal R. B., Sim A. T., Gonçalves C. A. and Dunkley P. R. (2002) Tyrosine hydroxylase dephosphorylation by protein phosphatase 2A in bovine adrenal chromaffin cells. *Neurochem. Res.* **27**, 207–213.
- Lehmann I. T., Bobrovskaya L., Gordon S. L., Dunkley P. R. and Dickson P. W. (2006) Differential regulation of the human tyrosine hydroxylase isoforms via hierarchical phosphorylation. *J. Biol. Chem.* **281**, 17644–17651.
- Lindgren N., Xu Z.-Q. D., Herrera-Marschitz M., Haycock J., Hökfelt T. and Fisone G. (2001) Dopamine D2 receptors regulate tyrosine hydroxylase activity and phosphorylation at Ser40 in rat striatum. *Eur. J. Neurosci.* **13**, 773–780.
- Lindgren N., Goiny M., Herrera-Marschitz M., Haycock J. W., Hökfelt T. and Fisone G. (2002) Activation of extracellular signal-regulated kinases 1 and 2 by depolarization stimulates tyrosine hydroxylase phosphorylation and dopamine synthesis in rat brain. *Eur. J. Neurosci.* **15**, 769–773.
- Luo Y., Liu B., Yang X., Ma X., Zhang X., Bragin D. E., Yang X. O., Huang W. and Liu M. (2017) Myeloid adrenergic signaling via CaMKII forms a feedforward loop of catecholamine biosynthesis. *J. Mol. Cell Biol.* **9**, 422–434.
- Mackintosh C. (2004) Dynamic interactions between 14-3-3 proteins and phosphoproteins regulate diverse cellular processes. *Biochem. J.* **381**, 329–42.
- Mils V., Baldin V., Goubin F., Pinta I., Papin C., Wayne M., Eychene A. and Ducommun B. (2000) Specific interaction between 14-3-3 isoforms and the human CDC25B phosphatase. *Oncogene* **19**, 1257–65.
- Moy L. Y. and Tsai L. H. (2004) Cyclin-dependent kinase 5 phosphorylates serine 31 of tyrosine hydroxylase and regulates its stability. *J. Biol. Chem.* **279**, 54487–54493.
- Nagatsu T., Levitt M. and Udenfriend S. (1964) Tyrosine hydroxylase the initial step in norepinephrine biosynthesis. *J. Biol. Chem.* **239**, 2910–2917.
- Nishi H., Demir E. and Panchenko A. R. (2015) Crosstalk between signaling pathways provided by single and multiple protein phosphorylation sites. *J. Mol. Biol.* **427**, 511–20.
- Obsilova V., Nedbalkova E., Silhan J., Boura E., Herman P., Vecer J., Sulc M., Teisinger J., Dyda F. and Obsil T. (2008) The 14-3-3 protein affects the conformation of the regulatory domain of human tyrosine hydroxylase. *Biochemistry* **47**, 1768–1777.
- Plattner F., Hayashi K., Hernández A., Benavides D. R., Tassin T. C., Tan C. and Day J. (2015) The role of ventral striatal cAMP signaling in stress-induced behaviors. *Nat. Neurosci.* **18**, 1094.
- Ramshaw H., Xu X., Jaehne E. J., et al (2013) Locomotor hyperactivity in 14-3-3 $\zeta$  KO mice is associated with dopamine transporter dysfunction. *Transl Psychiatry.* **3**, e327.
- Rodríguez-Pascual F., Ferrero R., Miras-Portugal M. T. and Torres M. (1999) Phosphorylation of tyrosine hydroxylase by cGMP-dependent protein kinase in intact bovine chromaffin cells. *Arch. Biochem. Biophys.* **366**, 207–14.
- Roskoski R., Vulliet P. R. and Glass D. B. (1987) Phosphorylation of tyrosine hydroxylase by cyclic GMP-dependent protein kinase. *J. Neurochem.* **48**, 840–845.
- Salvatore M. F. and Pruett B. S. (2012) Dichotomy of tyrosine hydroxylase and dopamine regulation between somatodendritic and terminal field areas of nigrostriatal and mesoaccumbens pathways. *PLoS ONE* **7**, e29867.
- Salvatore M. F., Garcia-Espana A., Goldstein M., Deutch A. Y. and Haycock J. W. (2000) Stoichiometry of tyrosine hydroxylase phosphorylation in the nigrostriatal and mesolimbic systems in vivo. *J. Neurochem.* **75**, 225–232.
- Salvatore M. F., Waymire J. C. and Haycock J. W. (2001) Depolarization-stimulated catecholamine biosynthesis: involvement of protein kinases and tyrosine hydroxylase phosphorylation sites in situ. *J. Neurochem.* **79**, 349–360.
- Skjevik Å. A., Mileni M., Baumann A., Halskau Ø., Teigen K., Stevens R. C. and Martinez A. (2014) The N-terminal sequence of tyrosine hydroxylase is a conformationally versatile motif that binds 14-3-3 proteins and membranes. *J. Mol. Biol.* **426**, 150–168.
- Sura G. R., Daubner S. C. and Fitzpatrick P. F. (2004) Effects of phosphorylation by protein kinase A on binding of catecholamines to the human tyrosine hydroxylase isoforms. *J. Neurochem.* **90**, 970–978.
- Sutherland C., Alterio J., Campbell D. G., Bourdelles B., Mallet J., Haavik J. and Cohen P. (1993) Phosphorylation and activation of human tyrosine hydroxylase in vitro by mitogen-activated protein (MAP) kinase and MAP-kinase-activated kinases 1 and 2. *Eur. J. Biochem.* **217**, 715–722.
- Toska K., Kleppe R., Armstrong C. G., Morrice N. A., Cohen P. and Haavik J. (2002) Regulation of tyrosine hydroxylase by stress-activated protein kinases. *J. Neurochem.* **83**, 775–783.
- Wang J., Lou H., Pedersen C. J., Smith A. D. and Perez R. G. (2009a) 14-3-3 $\zeta$  contributes to tyrosine hydroxylase activity in MN9D cells localization of dopamine regulatory proteins to mitochondria. *J. Biol. Chem.* **284**, 14011–14019.
- Wang S. Z., Sura G. R., Dangott L. J. and Fitzpatrick P. F. (2009b) Identification by hydrogen/deuterium exchange of structural changes in tyrosine hydroxylase associated with regulation. *Biochemistry* **48**, 4972–4979.
- Yamauchi T., Nakata H. and Fujisawa H. (1981) A new activator protein that activates tryptophan 5-monoxygenase and tyrosine 3-monoxygenase in the presence of Ca<sup>2+</sup>, calmodulin-dependent protein kinase. *Purification and characterization.* *J. Biol. Chem.* **256**, 5404–5409.

## Open Practices Disclosure

**Manuscript Title: Serine 19 phosphorylation and 14-3-3 binding regulate phosphorylation and dephosphorylation of tyrosine hydroxylase on serine 31 and serine 40**  
**Corresponding Author: Rune Kleppe**

Articles accepted to *Journal of Neurochemistry* after 01.2018 are eligible to earn badges that recognize open scientific practices: publicly available data, material, or preregistered research plans. Please read more about the badges in our *author guidelines and Open Science Badges page*, and you can also find information on the Open Science Framework [wiki](#).

Please check this box if you are interested in participating.

To apply for one or more badges acknowledging open practices, please check the box(es) corresponding to the desired badge(s) below and provide the information requested in the relevant sections. To qualify for a badge, you must provide a URL, doi, or other permanent path for accessing the specified information in a public, open-access repository. **Qualifying public, open-access repositories are committed to preserving data, materials, and/or registered analysis plans and keeping them publicly accessible via the web in perpetuity.** Examples include the Open Science Framework ([OSF](#)) and the various Dataverse networks. Hundreds of other qualifying data/materials repositories are listed at <http://re3data.org/>. Preregistration of an analysis plan must take place via a publicly accessible registry system (e.g., [OSF](#), [ClinicalTrials.gov](#) or other trial registries in the [WHO Registry Network](#), institutional registration systems). **Personal websites and most departmental websites do not qualify as repositories.**

Authors who wish to publicly post third-party material in their data, materials, or preregistration plan must have the proper authority or permission agreement in order to do so.

There are circumstances in which it is not possible or advisable to share any or all data, materials, or a research plan publicly. For example, there are cases in which sharing participants' data could violate confidentiality. If you would like your article to include an explanation of such circumstances and/or provide links to any data or materials you have made available—even if not under conditions eligible to earn a badge—you may write an alternative note that will be published in a note in the article. Please check this box if you would like your article to include an alternative note and provide the text of the note below:

**Alternative note:**

## Open Data Badge

1. Provide the URL, doi, or other **permanent path** for accessing the data in a **public, open-access repository**:

Confirm that there is sufficient information for an independent researcher to reproduce **all of the reported results**, including codebook if relevant.

Confirm that you have registered the uploaded files so that they are **time stamped** and cannot be age.

## Open Materials Badge

1. Provide the URL, doi, or other **permanent path** for accessing the materials in a **public, open-access repository**: all relevant information is provided in the manuscript and custom-made materials will be provided upon reasonable request.

Confirm that there is sufficient information for an independent researcher to reproduce **all of the reported methodology**.

Confirm that you have registered the uploaded files so that they are **time stamped** and cannot be age.

## Preregistered Badge

1. Provide the URL, doi, or other **permanent path** to the registration in a **public, open-access repository\***:
2. Was the analysis plan registered prior to examination of the data or observing the outcomes? If no, explain.\*\*
3. Were there additional registrations for the study other than the one reported? If yes, provide links and explain.\*

\*No badge will be awarded if (1) is not provided, or if (3) is answered "yes" without strong justification

\*\*If the answer to (2) is "no," the notation DE (Data Exist) will be added to the badge, indicating that registration postdates realization of the outcomes but predates analysis.

By printed date and name (handwritten) below, authors affirm that the above information is accurate and complete, that any third-party material has been reproduced or otherwise made available only with the permission of the original author or copyright holder, and that publicly posted data do not contain information that would allow individuals to be identified without consent.

***Please do not add you signature to avoid any misuse, as this form will be published with the manuscript.***

Date:

9. September, 2019

Handwritten Name (\*not\* signature):

